Tetrahedron 100 (2021) 132481

Contents lists available at ScienceDirect

Tetrahedron

journal homepage: www.elsevier.com/locate/tet

Extended porphyrinoid chromophores: heteroporphyrins fused to phenanthrene and acenaphthylene

Timothy D. Lash*, Patrick J. Rauen

Department of Chemistry, Illinois State University, Normal, IL, 61790-4160, USA

ARTICLE INFO

Article history:
Received 11 August 2021
Received in revised form
19 September 2021
Accepted 28 September 2021
Available online 2 October 2021

Keywords:
Core modified porphyrins
Heteroporphyrins
Conjugation
Aromaticity

ABSTRACT

Fusion of aromatic subunits onto porphyrin chromophores produces variable results and in some cases only minor bathochromic shifts are observed. In order to extend these observations, a series of oxa-, thia- and selenaporphyrins with fused acenaphthylene or phenanthrene units have been synthesized. Phenanthro[5,6-*b*]porphyrins were previously prepared via conventional '2 + 2' MacDonald condensations, but a more versatile '3 + 1' synthesis is now reported. Phenanthrotripyrranes reacted with a pyrrole dialdehyde in the presence of trifluoroacetic acid, followed by an oxidation step, to give phenanthroporphyrins. However, this chemistry initially gave products that were contaminated with isomeric impurities. Fortunately, good yields of isomerically pure phenanthroporphyrins were obtained when the reactions were carried out under relatively concentrated conditions, and a diphenanthroporphyrin was also obtained using this strategy. An alternative '3 + 1' synthesis was performed where a phenanthropyrrole dialdehyde was condensed with a tripyrrane and this also afforded a phenanthroporphyrin in good yields. Furan, thiophene and selenophene dialdehydes similarly reacted with phenanthro- and acenaphthotripyrranes to give a series of heteroporphyrins with fused phenanthrene and acenaphthylene rings. All of these porphyrinoids retained highly diatropic characteristics. As is the case for tetrapyrrolic porphyrins, the presence of a fused acenaphthylene unit leads to highly modified UV–vis spectra with multiple Soret bands and relatively strong Q bands above 650 nm. However, the longest wavelength absorptions for the acenaphthylene series were only red shifted by 12–15 nm compared to the phenanthrene-fused heteroporphyrin series, which is a somewhat reduced effect compared to previously reported phenanthroporphyrins and acenaphthoporphyrins. Nevertheless, the combined effects of core modification and acenaphthylene ring fusion affords potentially valuable strongly red shifted absorption bands between 677 and 684 nm.

1. Introduction

Investigations into the synthesis of porphyrins with strong absorptions in the red or far red regions has received a considerable amount of attention due to potential applications ranging from photodynamic therapy [1] to the construction of dye sensitized solar cells and chemical sensors [2]. Although fusion of aromatic rings to porphyrin chromophores can have desirable effects, the influence of the fused rings is highly structure dependent [3–6]. Fusion of a benzene ring to one of the pyrrolic units to give benzoporphyrin **1** produces minor bathochromic shifts [7], while naphtho[1,2-*b*]porphyrins **2** [8], phenanthro[5,6-*b*]porphyrins **3** [9,10], pyreno[4,5-*b*]porphyrins **4** [11], fluoranthoporphyrins **5** [12] and even corannulenoporphyrins **6** [13] (Fig. 1) only show small additional shifts to longer wavelengths [14]. The Soret bands for **1**–**6** appear at 403, 415, 417, 421, 436 and 429 nm, respectively, while the longest wavelength Q bands (Q1) show up at 628, 630, 634, 636, 634 and 644 nm. Given that octaalkylporphyrins typically give Soret bands near 400 nm and Q1 bands at 622 nm, these shifts are surprisingly small [4]. Larger effects can be obtained by introducing more than one fused ring [4], and linearly annealed naphthalene [15] and anthracene [16] units may also produce larger shifts, but for the most part the bathochromic shifts resulting from the introduction of large fused π-systems are small. Fusion of heteroaromatic rings such as quinoline [17], isoquinoline [17] and phenanthroline [18] also resulted in minor shifts. However, benzothiadiazole-fused porphyrins [19,20] and closely related systems [21,22] such as **7** showed much larger effects producing

* Corresponding author.
E-mail address: tdlash@ilstu.edu (T.D. Lash).

https://doi.org/10.1016/j.tet.2021.132481
0040-4020/

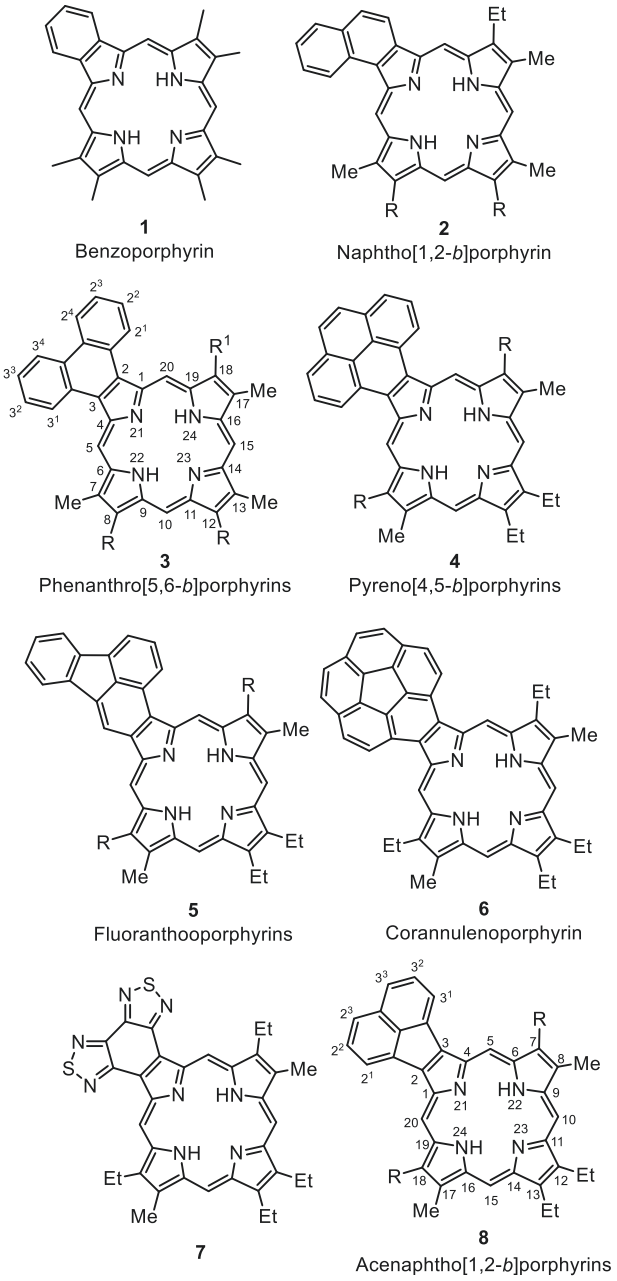

Fig. 1. Selected annulated porphyrin structures.

highly modified electronic spectra, although this still did not result in the production of long wavelength Q band absorptions. During the course of our investigations, porphyrins with fused acenaphthylene rings (e.g. **8**) were synthesized [20,23,24]. In stark contrast to the results noted above, acenaphthylene induced major changes giving rise to multiple Soret bands and producing a strong Q band at 658 nm. These effects were further magnified in diacenaphthoporphyrins and tetraacenaphthoporphyrins [20,24]. In addition, similar shifts were noted for acenaphthylene-fused sapphyrins [25], carbaporphyrins [26], oxybenziporphyrins [27] and oxypyriporphyrins [27]. Acenaphthoporphyrins have been investigated for applications as photosensitizers in photodynamic therapy (PDT) [28], and have shown promise in the treatment of leismaniasis [29]. Tetraacenaphthoporphyrins with naphthalene diimide subunits have also been applied to band gap engineering [30].

Heteroporphyrins (e.g. **9**–**11**, Scheme 1), core modified structures in which one of more of the nitrogen atoms have been replaced by other heteroatoms such as oxygen, sulfur and selenium, provide an alternative approach to modifying the porphyrin chromophore [31–33]. Although the first examples of heteroporphyrins were *meso*-unsubstituted structures [34], most of the work in this area has focused on *meso*-tetrasubstituted compounds [31]. Recently, we reported an improved '3 + 1' synthesis [35,36] of *meso*-unsubstituted oxa-, thia- and selenaporphyrins **9**–**11** [37], and this strategy was used to prepare internally alkylated derivatives (Scheme 1) [37]. This approach is well suited for the preparation of further modified structures and can in principle be applied to the preparation of heteroporphyrins with fused aromatic rings. In this work, two series of heteroporphyrins with fused phenanthrene and acenaphthylene rings are described and the resulting effects on these porphyrinoid chromophores are reported.

2. Results and discussion

Suitably substituted pyrroles **12** with fused aromatic rings can often be synthesized [38] by condensing nitroaromatic compounds **13** with isocyanoacetate esters in the presence of a non-nucleophilic base (Barton-Zard reaction [39]). These *c*-annulated pyrroles provide the starting point for the synthesis of ring fused porphyrin systems (Scheme 2) [36]. In our original syntheses of phenanthroporphyrins **3** [10], the macrocycle was constructed using the MacDonald '2 + 2' condensation (Scheme 3A) [36]. In this methodology, a dipyrrylmethane **14** was condensed with a dipyrrylmethane dialdehyde **15** in the presence of *p*-toluenesulfonic acid to give, following an oxidation step, phenanthroporphyrins **3** [10]. Acenaphthoporphyrins **8** were prepared using the more versatile '3 + 1' version of the MacDonald synthesis (Scheme 3B) in which acenaphthotripyrrane di-*tert*-butyl esters **16** were deprotected with trifluoroacetic acid (TFA) and immediately reacted with a pyrrole dialdehyde **17**. Following oxidation with 2,3-dichloro-5,6-dicyano-1,4-benzoquinone (DDQ), acenaphthoporphyrins **8** were isolated in 34–36% yield [20,23]. The '3 + 1' methodology was subsequently adapted for the synthesis of phenanthroporphyrins and the results for these studies are described below.

Phenanthropyrrole **18** [20] was refluxed with two equivalents of acetoxymethylpyrroles **19a,b** [40] in ethanol containing catalytic acetic acid [41,42] to give the corresponding phenanthrotripyrranes **20a,b** (Scheme 4). The terminal *tert*-butyl ester protective groups of **20a,b** can be cleaved with trifluoroacetic acid (TFA) at room temperature and the resulting deprotected intermediates can then be condensed with pyrrole dialdehydes. Using TFA as a catalyst, this methodology generally affords isomerically pure porphyrin products. However, some problems were encountered using phenanthrotripyrranes **20a,b**. When 100 mg of **20a** was reacted with 1 molar equivalent of pyrrole dialdehyde **17** in the presence of TFA in

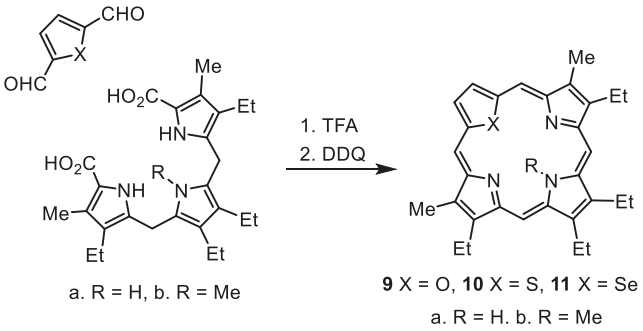

Scheme 1. Synthesis of *meso*-unsubstituted heteroporphyrins.

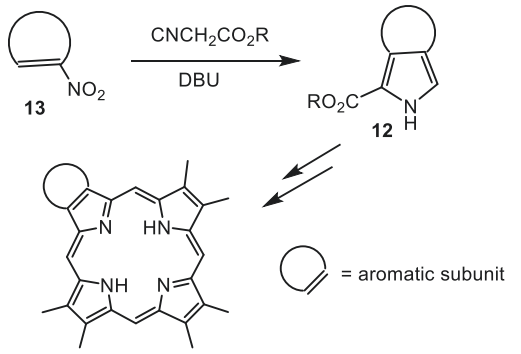

Scheme 2. Synthesis of *c*-annulated pyrroles.

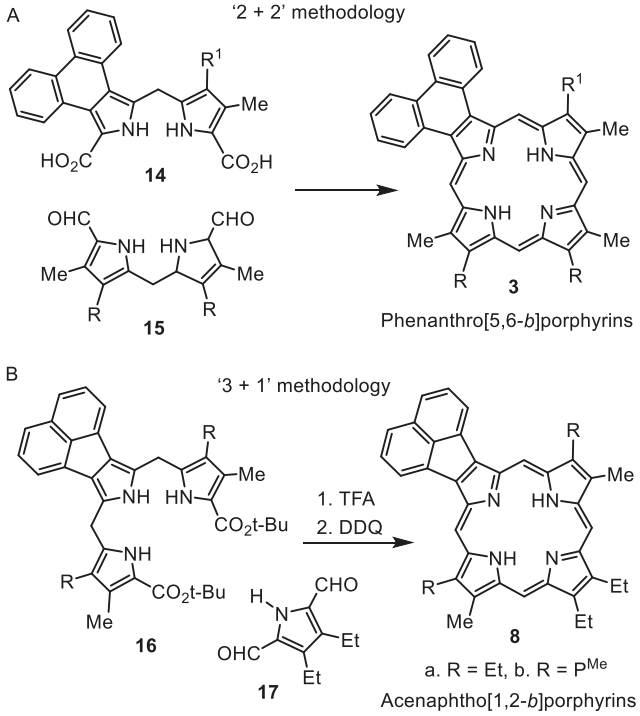

Scheme 3. '2 + 2' and '3 + 1' MacDonald syntheses of porphyrins with fused aromatic rings.

38 mL of dichloromethane, followed by oxidation with DDQ, the proton NMR spectrum for porphyrin product **21a** showed the presence of minor impurity peaks (Fig. 2). This problem can arise due to the ability of pyrrolic intermediates such as tripyrranes to undergo fragmentation-recombination reactions (Scheme 5) that can result in the formation of isomeric species [27,43]. In most organic reactions, the formation of large rings benefits from using dilute conditions as these favor intramolecular condensations rather than competing intermolecular reactions. However, these fragile pyrrolic intermediates may not survive intact under dilute conditions and lower yields of isomerically impure porphyrin products may be produced. Once the condensations have taken place, the products, often dihydroporphyrins, are far more stable and are no longer prone to rearrangements. Taking this into account, the volume of solvent was reduced to 15 mL and these conditions gave the desired isomerically pure phenanthroporphyrin **21a** in 57% yield (Fig. 2). Tripyrrane **20b** proved to be even more problematic, but pure phenanthroporphyrin **21b** could be obtained from **20b** and dialdehyde **17** when the solvent volume

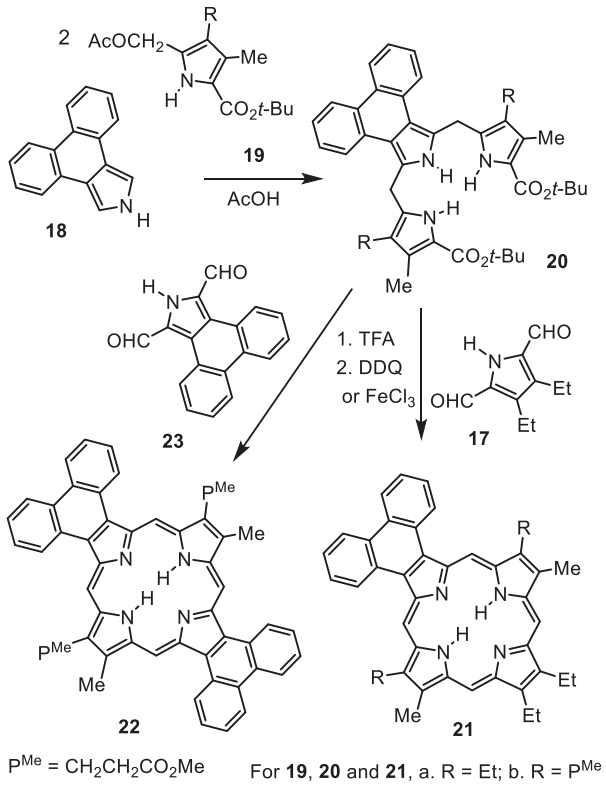

Scheme 4. '3 + 1' syntheses of phenanthro- and diphenanthroporphyrins.

was reduced to 5 mL. A diphenanthroporphyrin **22** was obtained under the same conditions from phenanthropyrrole dialdehyde **23** and tripyrrane **20b** in 40% yield.

An alternative '3 + 1' synthesis of monophenanthroporphyrin **24** was also carried out by reacting dialdehyde **23** with tripyrrane **25** in the presence of TFA, followed by oxidation with DDQ. In this case, the pure porphyrin was isolated in 58% yield (Scheme 6). Although **21a,b**, **22** and **24** are new compounds, they closely resemble previously reported phenanthroporphyrins and had similar spectroscopic properties [10]. However, it is notable that the UV–vis spectra of phenanthroporphyrins such as **21a** differ considerably from the analogous acenaphthoporphyrins, in this case **8a** (Fig. 3). Phenanthroporphyrin **21a** gives rise to a strong Soret band at 416 nm and affords a very weak Q1 band at 634 nm, while acenaphthoporphyrin **8a** produces multiple medium-intensity absorptions in the Soret band region and has a relatively strong Q band at 658 nm (Fig. 3).

Acenaphthopyrroles **26** (Scheme 7) are convenient precursors to acenaphthoporphyrins and related systems. These intermediates can in turn be prepared by reacting 1-nitroacenaphthylene (**27**) with isocyanoacetate esters **28** in the presence of the non-nucleophilic base 1,8-diazabicyclo[5.4.0]undec-7-ene (DBU) [20,23]. Nitration of acenaphthylene was achieved by reacting technical grade acenaphthylene with nitryl chloride by adapting a report by Iida et al. [45] to give **27**. This previously unreported procedure is provided in the experimental section. Following cleavage of the ester units, acenaphthopyrrole **29** was converted into the required tripyrrane intermediates (e.g. **30**) (Scheme 8).

Acenaphthoporphyrins have previously been synthesized from acenaphthotripyrrane di-*tert*-butyl esters [20]. However, tripyrrane dibenzyl esters are more commonly used intermediates in the synthesis of porphyrins and related systems. An advantage of these dibenzyl ester intermediates is that they often precipitate out from

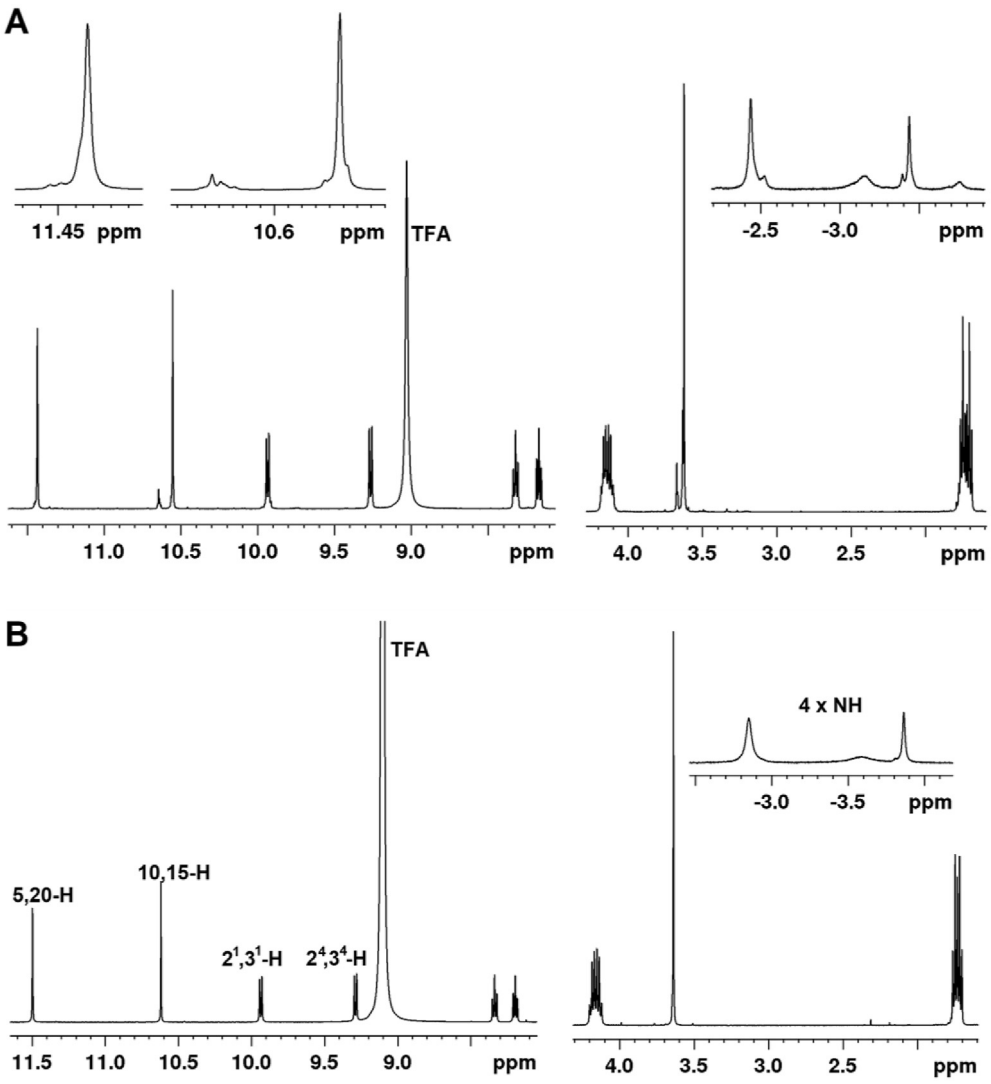

Fig. 2. 500 MHz NMR spectra of phenanthroporphyrin **21a** in TFA-$CDCl_3$. Spectrum A shows the spectrum for **21a** that is contaminated with isomeric impurities. Spectrum B corresponds to isomerically pure **21a** prepared under more concentrated conditions.

reaction mixtures, thereby simplifying purification [41]. With this in mind, the synthesis of acenaphthotripyrrane dibenzyl ester **30a** was considered as an alternative precursor to acenaphthoporphyrinoids. Acenaphthopyrrole **29** was heated with acetoxymethylpyrrole **31** in ethanol containing acetic acid and pure tripyrrane **30a** precipitated from solution in 77% yield (Scheme 8). The proton NMR spectrum of **30a** in $CDCl_3$ (Fig. 4A) showed features that are typical of tripyrrane dibenzyl esters. The methylene units of the benzyl esters gave broad peaks atypically shifted upfield to 4.5 ppm. In addition, the aromatic protons for the benzyl units were significantly shifted upfield, particularly in the case of the *ortho*-protons which appear at 6.8 ppm, approximately 0.5 ppm upfield from the expected value. Furthermore, the bridging methylene moieties gave rise to very broad signals. At higher temperatures (Fig. 4B) the resonances sharpen up but the abnormal chemical shifts are retained. These results suggest that the tripyrrane takes on a helical conformation where the terminal substituents are deshielded by the π-electrons at the opposite ends of the molecule [46,47]. Helical systems are chiral and would therefore give rise to diastereotopic protons. When helix-to-helix interconversion is rapid, these protons will effectively have equivalent chemical environments, but at lower temperatures this effect leads to peak broadening and the diastereotopic protons can potentially resolve into separate resonances. Tripyrrane dibenzyl esters that exhibit modified proton NMR spectra of the type described above have been shown to give good yields of porphyrin-type products [46,47]. However, when substituents are introduced that disrupt the proposed helical geometry, the yields of porphyrinoid products are greatly reduced [45,46]. However, it should be noted that solvent effects may also alter the conformations of these systems. Specifically, when the proton NMR spectrum of tripyrrane **30a** was obtained in DMSO-d_6, the resonances showed none of the shifts associated with the helical structure. This is presumably due to the solvent hydrogen bonding to the pyrrolic NH's, thereby disrupting the helical conformation. It is also worth noting that tripyrrane di-*tert*-butyl esters do not exhibit these types of shifts, but these tripyrrolic intermediates are still effective intermediates. MacDonald-type condensations involve the reaction of deprotected intermediates and so long as these can take on a helical geometry, macrocyclic ring closure can take place. Therefore, the absence of helical conformations in tripyrrane di-*tert*-butyl esters does not present a problem. Hydrogenolysis of the benzyl esters in **30a** over 10% palladium-charcoal afforded the corresponding dicarboxylic acid **30b** and this was reacted with pyrrole dialdehyde **17** to give

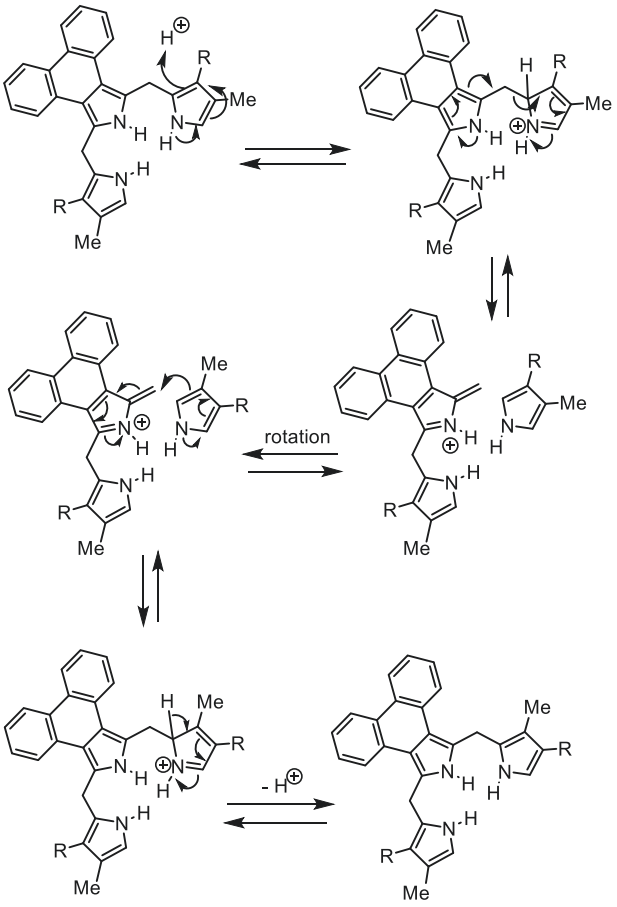

Scheme 5. Mechanism for the acidolytic fragmentation-recombination of phenanthrotripyrranes leading to isomeric byproducts.

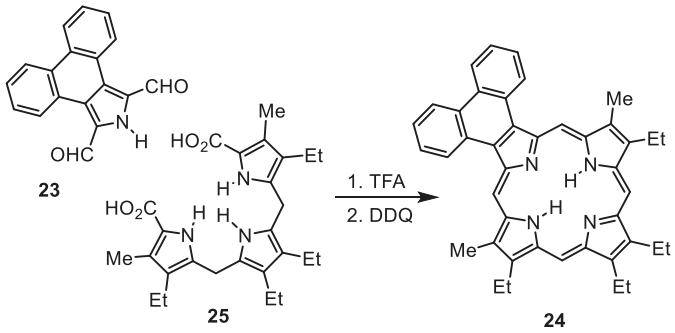

Scheme 6. Alternative '3 + 1' synthesis of a phenanthroporphyrin.

acenaphthoporphyrin **8a**. Comparable yields were obtained to those previously reported (Scheme 3B), and there appears to be no particular advantage to using **30a** instead of di-*tert*-butyl ester **16a**. For this reason, most of our investigations made use of **16a**.

Having laid the foundations for further studies in this area, the synthesis of core modified porphyrinoids with fused phenanthrene and acenaphthylene units could now be attempted. Recently, we reported an improved synthesis of *meso*-unsubstituted oxa- and thiaporphyrins, **9** and **10**, together with the first examples of *meso*-unsubstituted selenaporphyrins **11** (Scheme 1), and this strategy provided access to the first examples of *N*-alkyl heteroporphyrins [37]. Given the success of these investigations, together with the availability of phenanthro- and acenaphthotripyrranes, '3 + 1'

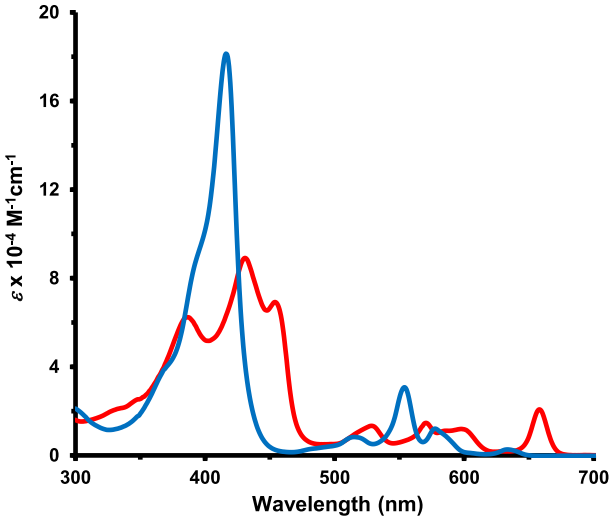

Fig. 3. UV–vis spectra of acenaphthoporphyrin **8a** (red line) and phenanthroporphyrin **21a** (blue line) in 1% Et_3N–$CHCl_3$.

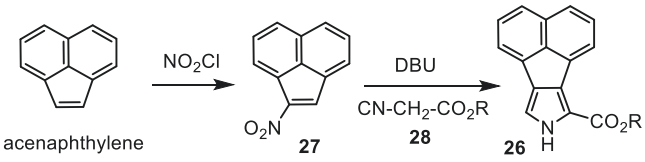

Scheme 7. Synthesis of acenaphthopyrrole esters.

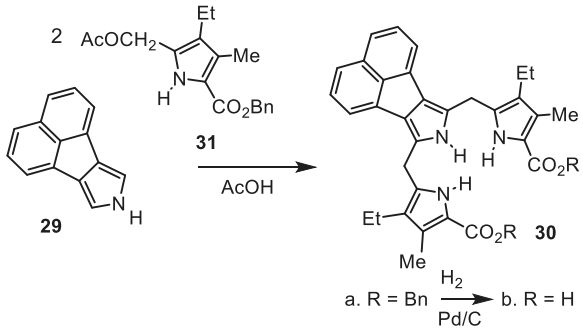

Scheme 8. Synthesis of an acenaphthotripyrrane.

syntheses of annulated heteroporphyrins **32** and **33** (Schemes 9 and 10) were investigated. In order to provide a matched set of porphyrinoid structures, phenanthroporphyrin **34** and acenaphthoporphyrin **35** were also prepared with an unsubstituted pyrrole unit that matched the similarly unsubstituted furan, thiophene and selenophene moieties in **32a-c** and **33a-c**. As phenanthrotripyrranes are more prone to rearrangement than other intermediates of this type (see above), relatively concentrated reaction conditions were used to prepare phenanthro[5,6-*l*]-21-heteroporphyrins **32** (Scheme 9). Following deprotection of tripyrrane di-*tert*-butyl ester **20a** with TFA, reaction with 2,5-pyrroledicarbaldehyde (**36**) [48] and oxidation with DDQ gave phenanthroporphyrin **34** in 37% yield. Heteroporphyrins **32** were similarly prepared by reacting furan [49], thiophene or selenophene [50] dialdehydes **37a-c** with tripyrrane **20a** in the presence of TFA, and subsequent oxidation with aqueous ferric chloride [25b,51], gave **32a-c** in 54%, 38% and 30% yields, respectively. Less concentrated conditions were used to prepare

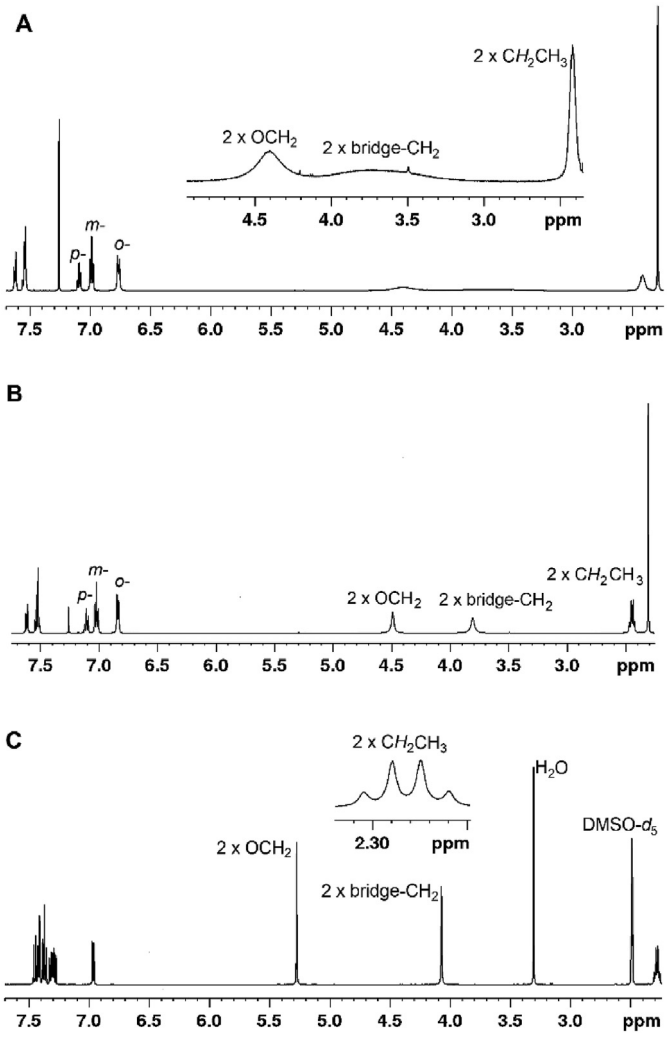

Fig. 4. Proton NMR spectra of acenaphthotripyrrane **31a**. A. **31a** in $CDCl_3$ at 32 °C. B. **31a** in $CDCl_3$ at 55 °C. C. **31a** in DMSO-d_6 at 32 °C.

heteroacenaphthoporphyrins **33a-c** (Scheme 10). Treatment of tripyrrane **16a** with TFA, followed by addition of dichloromethane and diformylpyrrole **36** and oxidation with DDQ afforded acenaphthoporphyrin **35** in 35% yield. Heteroacenaphthoporphyrins **33** were prepared similarly, using aqueous ferric chloride as the oxidant, and oxa-, thia- and selenaporphyrins **33a-c** were isolated in 64%, 28% and 23% yields, respectively (Scheme 10). All of the porphyrinoid products were purified by column chromatography, followed by recrystallization, and the molecular formulae were confirmed by high resolution mass spectrometry.

Due to the poor solubility of free base heteroporphyrins **32a-c** and **33a-c**, NMR data were obtained for the protonated forms in TFA-$CDCl_3$. The proton NMR spectra showed the presence of strong diamagnetic ring currents that are consistent with highly aromatic compounds. Fig. 5 shows the upfield and downfield regions in the proton NMR spectra for oxaporphyrins **32a** (A) and **33a** (B). In both cases, the *meso*-protons are shifted downfield beyond 11 ppm, and the furan protons are similarly deshielded, appearing near 10.5 ppm. The phenanthrene and acenaphthylene protons of the fused rings also exhibit significant downfield shifts, possibly indicating that the aromatic delocalization pathways can extend into the arene units. In phenanthro-oxaporphyrin the resonance at 9.98 ppm corresponds to the protons orientated towards the

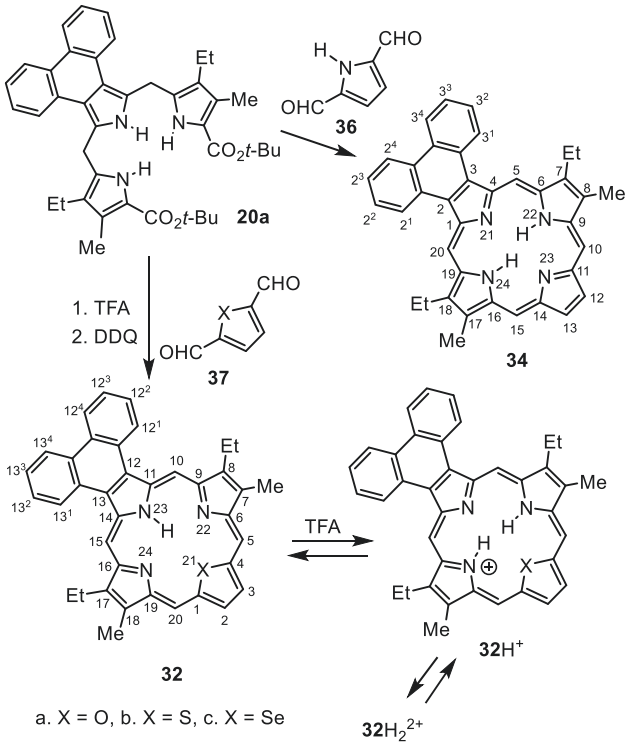

Scheme 9. Synthesis of phenanthrene-fused heteroporphyrins.

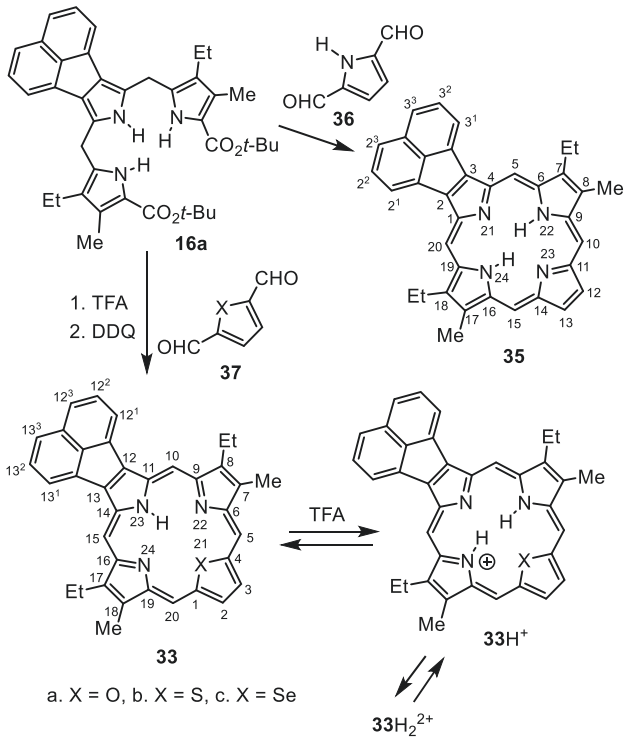

Scheme 10. Synthesis of acenaphthylene-fused heteroporphyrins.

macrocycle and anisotropy is in part responsible for the downfield shift. However, the remaining resonances show up at 8.26, 8.40 and 9.34 ppm, substantially downfield from the values observed in phenanthrene. Protonation is unlikely to be the direct cause of these shifts and it can be postulated that extended conjugation

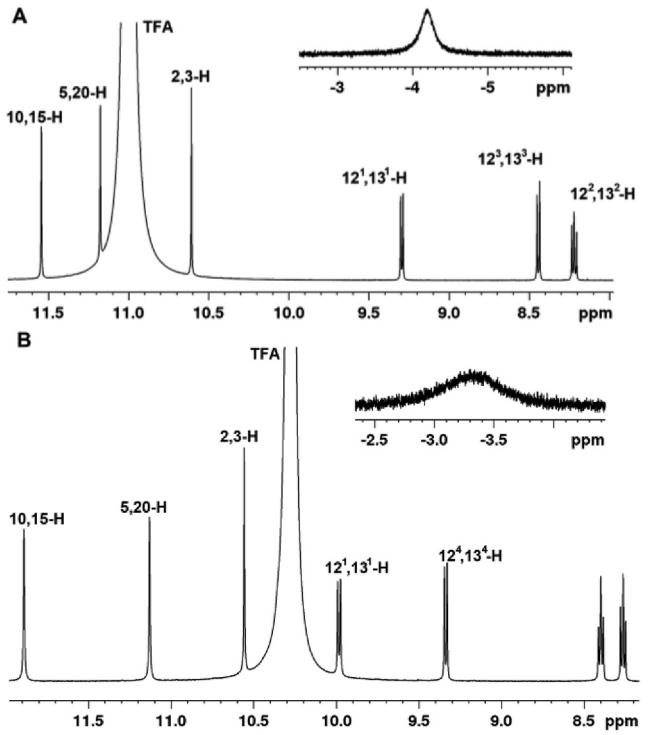

Fig. 5. Partial proton NMR spectra of oxa-acenaphthoporphyrin **33a** (A) and oxa-phenanthroporphyrin **32a** (B) in TFA-$CDCl_3$.

pathways can pass through the periphery of the fused rings as illustrated in structure **38** (Fig. 6). Similar effects are seen in protonated thia- and selenaphenanthroporphyrins **32b** and **32c** and in regular phenanthroporphyrins [10] such as **3** and **34**. Inspection of the proton NMR spectrum for protonated tetraphenanthroporphyrin **39** also shows strong deshielding for the phenanthrene protons [9]. However, it is less clear why similar deshielding effects are also observed for protonated acenaphthoporphyrins **8** [20] and **35** and heteroacenaphthoporphyrins **33**. These shifts are little altered by the presence of larger heteroatoms within the porphyrinoid cavity and the deshielding effects are virtually unchanged for selena-acenaphthoporphyrin **33c** in TFA-$CDCl_3$ (Fig. 7). A detailed investigation into the conjugation effects for these systems is currently in progress.

Further insights into these structures can be obtained from the electronic absorption spectra. Fig. 8 shows the UV–vis spectra for phenanthroporphyrin **34** and acenaphthoporphyrin **35**. The spectrum for **34** is similar to previously reported phenanthroporphyrins [10] with a strong Soret band 413 nm and a weak Q1 band at

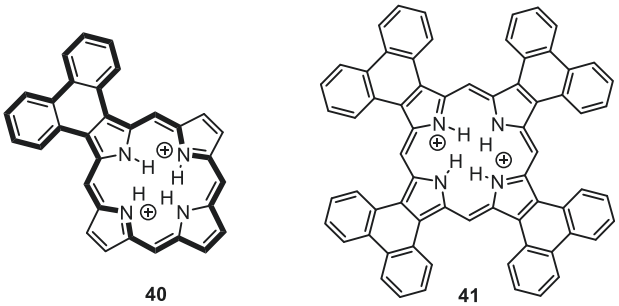

Fig. 6. Potential 30π electron delocalization pathway in diprotonated phenanthroporphyrins and the structure of a tetraphenanthroporphyrin dication.

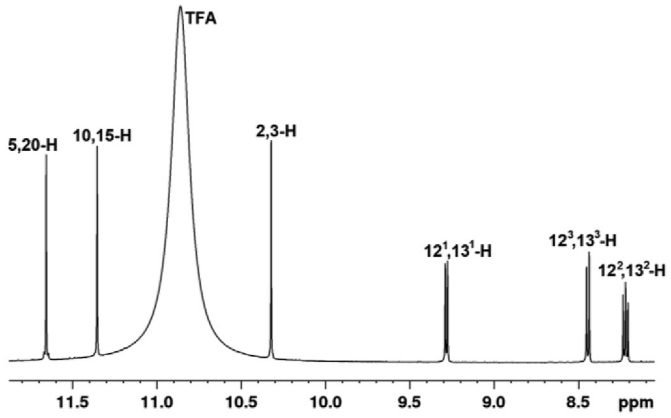

Fig. 7. Partial proton NMR spectrum of selena-acenaphthoporphyrin **33c** in TFA-$CDCl_3$.

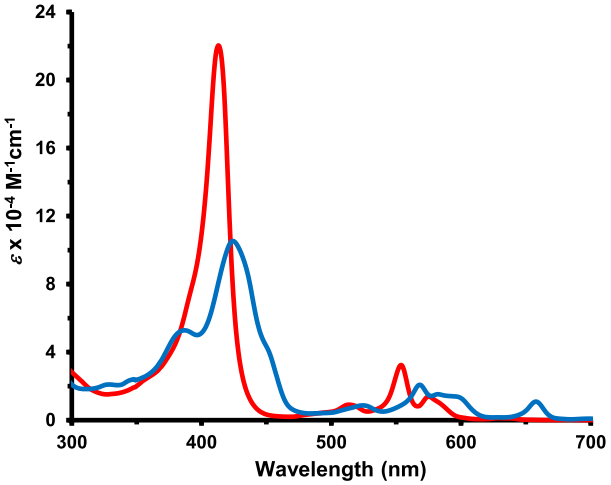

Fig. 8. UV–vis spectra of phenanthroporphyrin **34** (red line) and acenaphthoporphyrin **35** (blue line) in 1% Et_3N–$CHCl_3$.

628 nm. The Soret band region for acenaphthoporphyrin **35** is less typical, giving one primary, albeit weakened, Soret absorption, together with two shoulders. However, as is the case for other monoacenaphthoporphyrins [20], a moderately strong Q band is observed at 658 nm. Spectrophotometric titration of **34** with TFA showed the gradual formation of a new protonated species but little further change was observed at higher concentrations of TFA (Fig. 9). In 2% TFA-CH_2Cl_2, the Soret band appeared at 420 nm, while the longest wavelength Q band was present at 614 nm. Similar titrations of acenaphthoporphyrin **35** led to an intensification of the Soret band, which was bathochromically shifted to 442 nm, and the appearance of a long wavelength band at 627 nm (Fig. 10). Again, only minor changes were observed upon further addition of TFA. In both cases, the results are consistent with the direct formation of diprotonated species.

Oxaporphyrins **32a** and **33a** readily underwent protonation, but UV–vis spectra for the free base forms could be obtained in 1% triethylamine-CH_2Cl_2 (Fig. 11). The phenanthrene fused system gave a diminished Soret band at 422 nm and a series of weak Q bands extending to 662 nm. In contrast, acenaphtho-oxaporphyrin **33a** afforded three Soret bands at 383, 429 and 454 nm and a relatively strong Q band at 677 nm. In CH_2Cl_2 or $CHCl_3$, **32a** and **33a** both gave completely different spectra (Figs. 12 and 13) even when the solvents were passed through a column of basic alumina. These

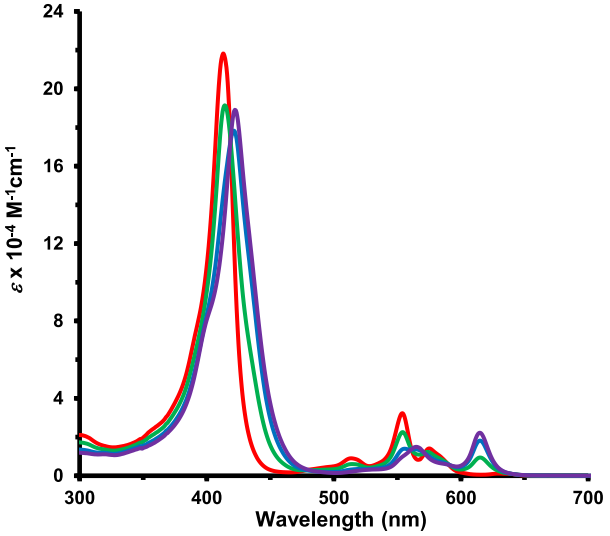

Fig. 9. UV–vis spectra of **34** in CH_2Cl_2 with 0 equiv (red), 10 equiv (green) 20 equiv (blue) and 50 equiv (purple) of TFA.

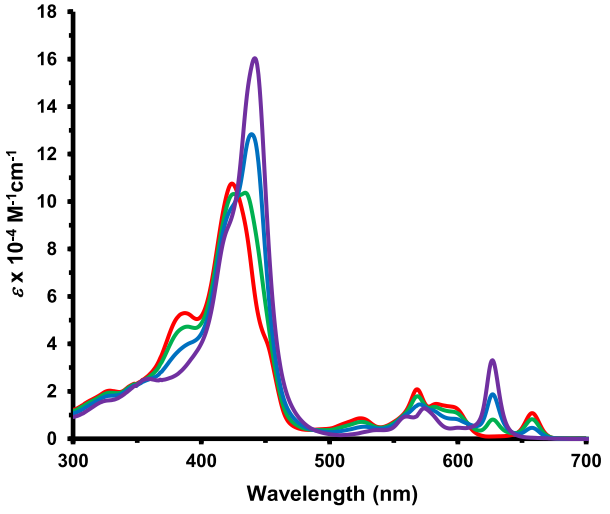

Fig. 10. UV–vis spectra of **35** in chloroform with 0 equiv (red), 5 equiv (green), 10 equiv (blue) and 50 equiv (purple) of TFA.

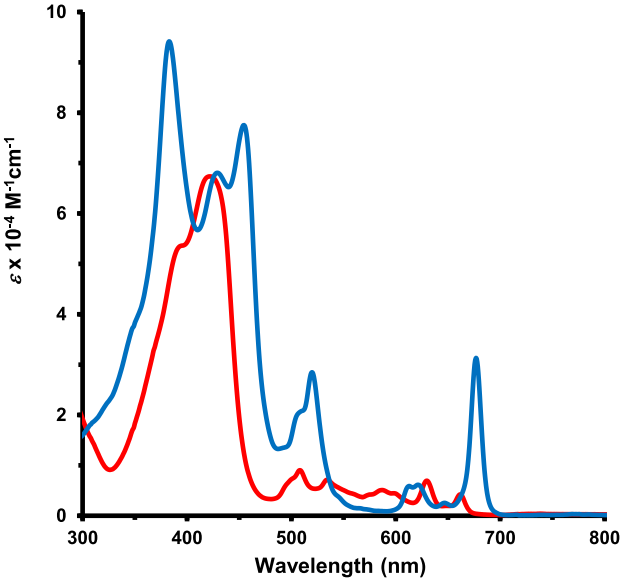

Fig. 11. UV–vis spectra of phenanthro-oxaporphyrin **32a** (red line) and acenaphtho-oxaporphyrin **33a** (blue line) in 1% Et_3N–CH_2Cl_2.

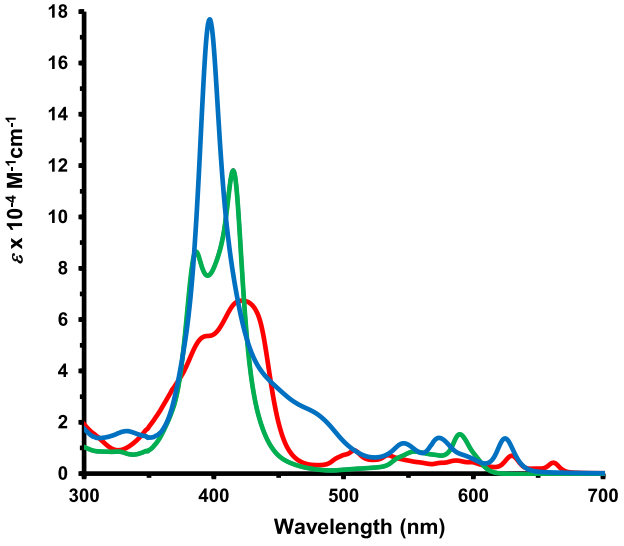

Fig. 12. UV–vis spectra of **32a** in 1% Et_3N–CH_2Cl_2 (red), in CH_2Cl_2 with 4 equiv TFA (green) and in 50% TFA-CH_2Cl_2 (blue).

were essentially unaltered in the presence of trace amounts of TFA. For **32a**, two Soret bands emerged at 386 and 416 nm. However, in 50% TFA a third species was observed with an intense Soret band at 397 nm (Fig. 12). These data indicate that at lower acid concentrations, a monoprotonated species **32a**H^+ is formed (Scheme 9), and that diprotonation only occurs under highly acidic conditions. Similar results were obtained for acenaphtho-oxaporphyrin **33a** (Fig. 13), although diprotonation appears to be complete in this case with 1% TFA-CH_2Cl_2. In the presence of low concentrations of TFA, a strong Soret band is observed at 424 nm and the longest wavelength Q band is present at 605 nm. However, in 5% TFA-CH_2Cl_2, weaker Soret bands are present between 350 and 450 nm, and the longest wavelength Q band appears at 639 nm.

The free base spectra for thiaporphyrins **32b** and **33b** show similar contrasts. In 1% Et_3N–CH_2Cl_2, phenanthro-thiaporphyrin **32b** gave a slightly broadened Soret band at 422 nm and a longest wavelength Q band at 669 nm, while acenaphtho-thiaporphyrin **33b** afforded three Soret absorptions at 389, 432 and 456 nm and the Q1 band at 682 nm (Fig. 14). Addition of TFA to **32b** led to the formation of a new species, assigned to monocation **32b**H^+, with Soret bands at 401 and 431 nm and a longest wavelength Q band at 611 nm (Fig. 15). At higher concentrations of TFA, a Soret band emerged at 421 nm and a longer wavelength band appeared at 647 nm, indicating that a diprotonated species **32b**H_2^{2+} had been generated. Addition of TFA to **33b** led to the formation of a strong Soret band at 424 nm and the longest wavelength Q band appeared at 605 nm (Fig. 16) corresponding to monocation **33b**H^+. In 1% TFA-CH_2Cl_2, a new species attributed to dication **33**H_2^{2+} was observed with Soret bands at 402 and 425 nm and a longer wavelength absorption at 639 nm.

Selenaporphyrin **32c** and **33c** provided further contrasts between the two series to be made (Fig. 17). Phenanthroselenaporphyrin **32c** gave a Soret band 428 nm and its longest

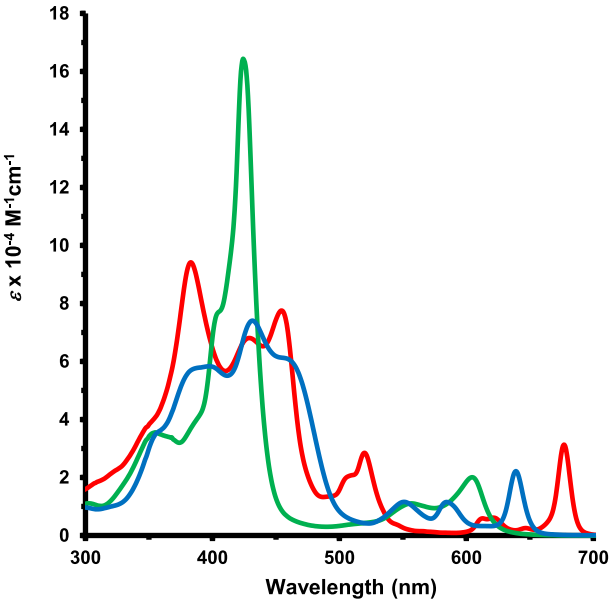

Fig. 13. UV–vis spectra of **33a** in 1% Et_3N–CH_2Cl_2 (red), in CH_2Cl_2 with 4 equiv TFA (green) and in 5% TFA-CH_2Cl_2 (blue).

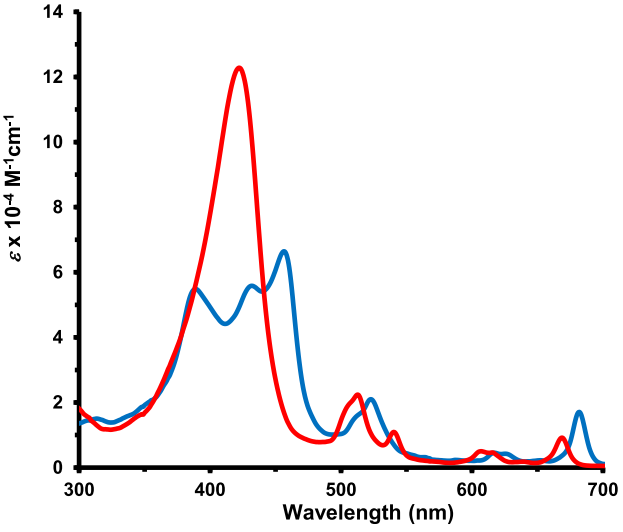

Fig. 14. UV–vis spectra of phenanthrothiaporphyrin **32b** (red) and acenaphthothiaporphyrin **33b** (blue) in 1% Et_3N–CH_2Cl_2.

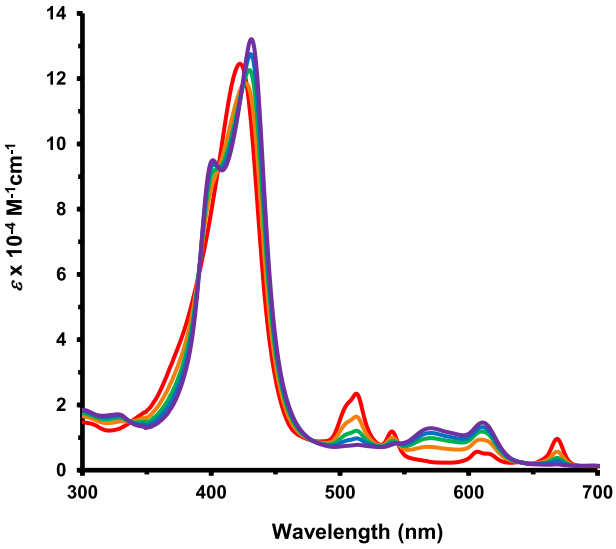

Fig. 15. UV–vis spectra of **32b** in CH_2Cl_2 with 0 equiv (red), 1 equiv (orange), 2 equiv (green), 3 equiv (blue), 5 equiv (purple) of TFA.

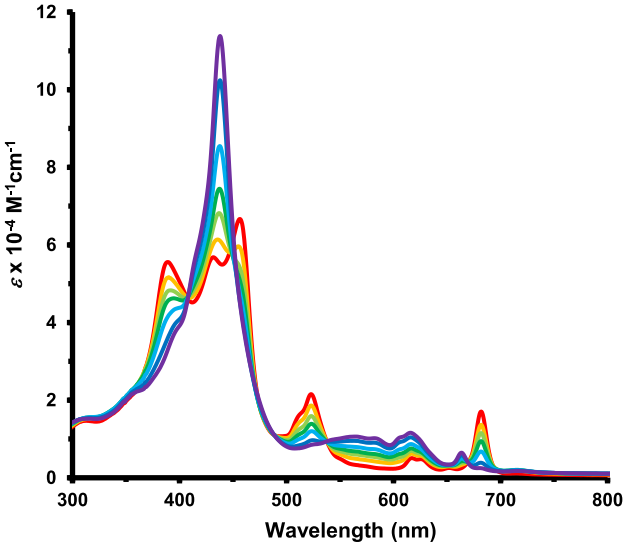

Fig. 16. UV–vis spectra of **33b** in CH_2Cl_2 with 0 equiv (red), 1 equiv (orange), 2 equiv (light green), 3 equiv (dark green), 5 equiv (light blue), 10 equiv (dark blue) and 20 equiv (purple) of TFA.

wavelength Q band appeared at 672 nm, while acenaphthoselenaporphyrin **33c** afforded three broad Soret absorptions and a longest wavelength Q band at 684 nm. Protonation of **32c** initially gave a species with a Soret band at 447 nm corresponding to monocation **32 c**H^+ (Fig. 18). In 20% TFA, a new species was evident with two very broad Soret bands at 402 and 486 nm and a long wavelength Q band at 617 nm. Addition of TFA to **33c** initially resulted in species with a Soret band at 464 nm, but further changes were noted at higher concentration of acid, including the emergence of Soret-like bands at 415 and 494 nm. Again, these changes can be attributed to the sequential formation of monocationic and dicationic species. In every case, heterophenanthro- and heteroacenaphthoporphyrins showed stepwise protonation processes, in contrast to porphyrins **34** and **35** which appeared to directly afford the dicationic species. Inhibition of the second protonation step for thia- and selenaporphyrins can be attributed to steric crowding within the macrocyclic cavity. The presence of an electronegative oxygen in oxaporphyrins **32a** and **33a** may also inhibit the second protonation step but monoprotonation occurs very easily for these structures (see Fig. 19).

The UV–vis spectra for the free base heteroporphyrins parallel the results obtained for tetrapyrrolic porphyrins [4] but some differences were noted. Acenaphthoheteroporphyrins **33a-c** all showed three weakened Soret bands, while phenanthrothia- and phenanthroselenaporphyrins **32b** and **32c** produced a single slightly broadened Soret band. Phenanthro-oxaporphyrin **32a** gave some additional complexity with two distinct shoulders in addition to the main Soret absorption. Of greater significance, heteroacenaphthoporphyrins gave relatively strong absorptions at longer wavelengths. Heteroporphyrins give bathochromic shifts that increase with the size of the heteroatom, and these combine with the

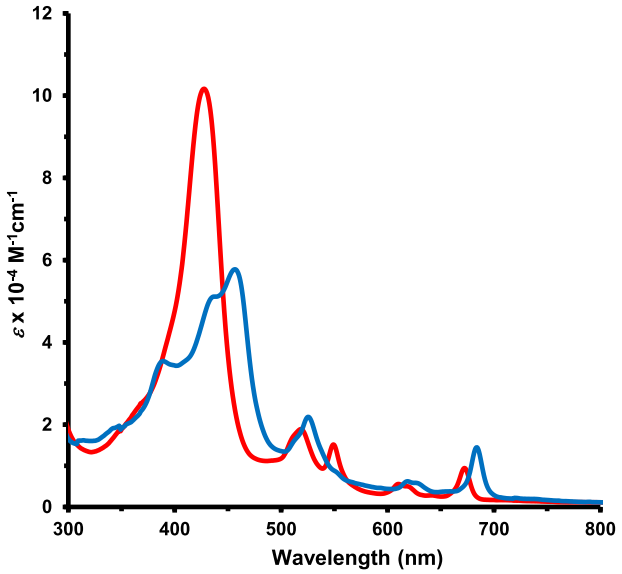

Fig. 17. UV–vis spectra of phenanthroselenaporphyrin **32c** (red) and acenaphthoselenaporphyrin **33c** (blue) in 1% Et_3N–$CHCl_3$.

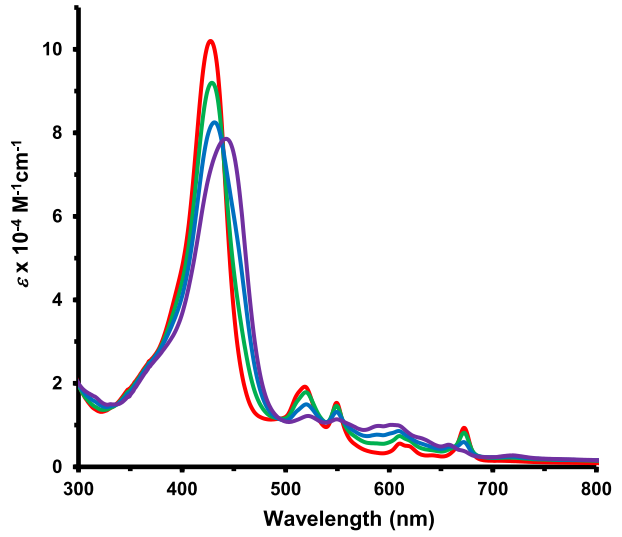

Fig. 18. UV–vis spectra of **32c** in $CHCl_3$ with 0 equiv (red), 50 equiv (green), 100 equiv (blue) and 200 equiv (purple) of TFA.

influence of the fused acenaphthylene unit to produce strong Q1 bands at 677 nm for **35a**, 682 nm for **35b** and 684 nm for **35c**. The Q1 bands for heterophenanthroporphyrins were of lower intensity and red shifted to a lesser extent. However, while this band is shifted to longer wavelengths by 30 nm in acenaphthoporphyrin **35** compared to phenanthroporphyrin **34**, the gap decreases to 15 nm for oxaporphyrins **32a** and **33a**, to 13 nm in thiaporphyrins **32b** and **33b**, and to 12 nm in selenaporphyrins **32c** and **33c**. Nevertheless, the relatively muted shifts in acenaphthoheteroporphyrins are counteracted by the comparative intensity of these peaks together with the additive effects of acenaphthylene ring fusion with core modification. Hence, these heteroporphyrins exhibit fairly intense absorptions in the longer wavelength region that could lead to applications.

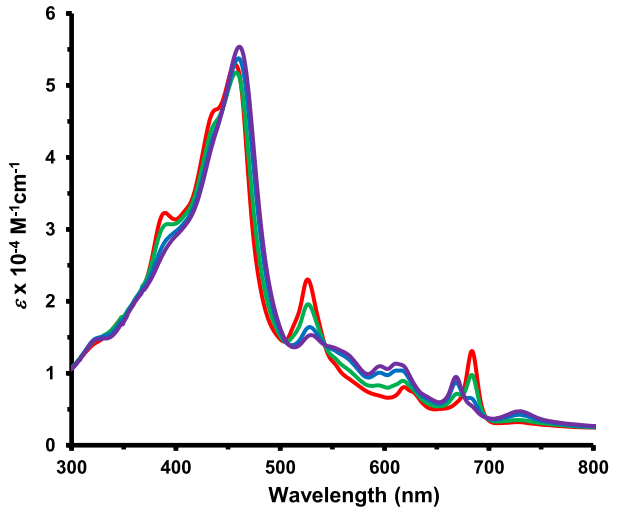

Fig. 19. UV–vis spectra of **33c** in $CHCl_3$ with 0 equiv (red), 100 equiv (green), 200 equiv (blue) and 400 equiv (purple) of TFA.

3. Conclusions

A series of phenanthroporphyrins, acenaphthoporphyrins and related heteroporphyrins have been synthesized by a '3 + 1' strategy from annulated tripyrranes. Phenanthrotripyrranes proved to be relatively prone to acidolytic scrambling but pure porphyrin and heteroporphyrin products could be isolated in good yields under high concentration conditions. Reaction of acenaphtho- and phenanthrotripyrranes with pyrrole, furan, thiophene and selenophene dialdehydes afforded matched sets of phenanthro- and acenaphthoporphyrinoids. Acenaphthoheteroporphyrins gave highly modified UV–vis spectra with moderately strong absorptions between 677 and 684 nm, showing that core modification increases the bathochromic shifts due to the presence of fused acenaphthylene units. In contrast, phenanthroheteroporphyrins showed much smaller shifts and relatively weak absorption bands at higher wavelengths.

4. Experimental

4.1. General

Acenaphthylene, 2,5-thiophenedicarbaldehyde, 2,3-dichloro-5,6-dicyano-1,4-benzoquinone (DDQ), trifluoroacetic acid and triethylamine were purchased from Aldrich or Acros, and were used without further purification. Chromatography was performed using grade 3 neutral alumina or 70–230 mesh silica gel. Melting points were determined in open capillary tubes on a Mel-Temp apparatus and are uncorrected. Proton and carbon-13 NMR data were obtained on a 500 MHz Bruker NMR spectrometer and were run at 302 K unless otherwise indicated. ^{1}H NMR values are reported as chemical shifts δ, relative integral, multiplicity (s, singlet; d, doublet; t, triplet; q, quartet; m, multiplet; br, broad peak) and coupling constant (J). Chemical shifts are reported in parts per million (ppm) relative to $CDCl_3$ (^{1}H residual $CHCl_3$ δ 7.26, ^{13}C $CDCl_3$ triplet δ 77.23 or DMSO-d_6 (^{1}H residual DMSO-d_5 pentet δ 2.49, ^{13}C DMSO-d_6 heptet δ 39.7), and coupling constants were taken directly from the spectra. NMR assignments were made with the aid of ^{1}H–^{1}H COSY, HSQC, DEPT-135, and NOE difference proton NMR spectroscopy. 2D experiments were performed by using standard software. ^{1}H and ^{13}C NMR spectra for all new compounds are reported in Supporting Information.

4.2. Synthetic procedures

4.2.1. 1-Nitroacenaphthylene (27) (with P. Chandrasekar)

This procedure was carried out in a well-ventilated fume hood. A 250 mL three-necked round bottom flask was equipped with a 50 mL addition funnel, a thermometer, and a Vigreux column with a still head attached to a condenser and a receiver flask containing 100 g of carbon tetrachloride. The receiver flask was cooled in a dry ice-acetone bath. Fuming nitric acid (10.0 g, 90% acid, 0.145 mol) was placed in the reaction vessel and cooled to 0 °C using a salt/ice bath. Fuming sulfuric acid (20% SO_3) was added dropwise to the stirred solution, while maintaining the temperature at 0 °C, and chlorosulfonic acid (16.89 g, 0.145 mol) was then added slowly via the addition funnel over a period of 2–3 h so that the temperature remained at 0 °C and no brown fumes were present in the reaction flask. Nitryl chloride was collected onto the frozen CCl_4 in the receiver flask as it was generated. After the addition of $ClSO_3H$ was complete, the cooling bath was removed, and the reaction mixture was stirred for an additional 15 min. The receiver flask, which was allowed to thaw to give a solution of NO_2Cl in CCl_4, showed a mass increase of 9.8 g (0.12 mol, 83%).

Commercially available acenaphthylene (31.58 g, 75% purity, 0.156 mol) was dissolved in carbon tetrachloride (100 mL) and cooled to 0 °C. A solution of NO_2Cl (9.8 g, 0.12 mol) in carbon tetrachloride (100 g) was added dropwise to the stirred acenaphthylene solution while maintaining the temperature at 0 °C. After the addition was complete, stirring was continued for a further 30 min. The solution was washed with 5% aqueous sodium bicarbonate solution (250 mL) and water (250 mL) and the aqueous solutions were back extracted with chloroform to minimize losses. The combined organic solutions were dried over sodium sulfate, filtered, and the solvents removed under reduced pressure. The solid residue was dissolved in a small amount of toluene, loaded onto a silica column, and eluted with hexanes. The first yellow fraction was discarded, and the product was then collected as an orange fraction. Evaporation of the solvent gave 1-nitroacenaphthylene (11.95 g, 60.6 mmol, 50%) as an orange powder, mp 122–123 °C (lit. mp [45] 124–125 °C). ^{1}H NMR (500 MHz, $CDCl_3$): δ 8.40 (1H, d, J = 7.0 Hz, 8-H), 8.10 (dd, 1H, J = 8.0, 0.6 Hz), 8.03 (s, 1H, 2-H), 8.01 (d, 1H, J = 7.0 Hz, 3-H), 7.97 (d, 1H, J = 8.2 Hz), 7.71–7.67 (m, 2H, 4,7-H). ^{13}C (125 MHz, $CDCl_3$): δ 149.1, 132.9, 132.8, 131.5, 130.6, 130.1, 129.8, 128.8, 128.7, 128.6, 128.1, 126.7.

4.2.2. Bis-1,3-(5-Benzyloxycarbonyl-3-ethyl-4-methyl-2-pyrrolylmethyl)acenaphtho[1,2-c]pyrrole (30a)

Acenaphthopyrrole **29** (0.25 g, 1.3 mmol) and acetoxymethylpyrrole **31** [52] (0.825 g, 2.6 mmol) were added to ethanol (15 mL) and acetic acid (1 mL) in a 25 mL round bottom flask. The mixture was purged with nitrogen and stirred under reflux for 16 h. The flask was cooled in an ice-water bath and the resulting precipitate was collected by suction filtration. Following drying *in vacuo*, the tripyrrane (0.71 g, 1.01 mmol, 77%) was obtained as a flaky off-white powder, mp 190–191 °C. ^{1}H NMR (500 MHz, $CDCl_3$): δ 11.46 (br s, 2H, 2 x NH), 9.20 (br s, 1H, NH), 7.64–7.61 (m, 2H), 7.56–7.53 (m, 4H) (6 x acenaphthylene-H), 7.09 (t, 2H, J = 7.4 Hz, 2 x p-H), 6.99 (t, 4H, J = 7.6 Hz, 4 x m-H), 6.77 (d, 4H, J = 7.5 Hz, 4 x o-H), 4.40 (v br, 4H, 2 x OCH_2), 3.71 (v br, 4H, 2 x bridge CH_2), 2.42 (br, 4H, 2 x pyrrole-CH_2), 2.29 (s, 6H, 2 x pyrrole-CH_3), 0.98 (t, 6H, J = 7.5 Hz, 2 x CH_2CH_3). ^{1}H NMR (500 MHz, $CDCl_3$, 55 °C): δ 10.80 (br s, 2H, 2 x NH), 8.82 (br s, 1H, NH), 7.68 (d, 2H, J = 8.1 Hz), 7.50 (t, 2H, J = 7.5 Hz), 7.43 (br d, 2H, J = 6.7 Hz), 7.12 (t, 2H, J = 7.3 Hz, 2 x p-H), 7.05 (t, 4H, J = 7.5 Hz, 4 x m-H), 6.90 (br d, 4H, J = 6.9 Hz, 4 x o-H), 4.61 (br s, 4H, 2 x OCH_2), 3.85 (br s, 4H, 2 x bridge CH_2), 2.43 (q, 4H, J = 7.5 Hz, 2 x pyrrole-CH_2), 2.30 (s, 6H, 2 x pyrrole-CH_3), 1.00 (t, 6H, J = 7.5 Hz, 2 x CH_2CH_3). ^{1}H NMR (500 MHz, DMSO-d_6): δ 11.30 (br s, 2H, 2 x NH), 10.35 (br s, 1H, NH), 7.45 (d, 2H, J = 8.2 Hz), 7.42 (d, 4H, J = 7.3 Hz, 4 x o-H), 7.37 (t, 4H, J = 7.3 Hz, 4 x m-H), 7.33–7.27 (m, 4H), 6.97 (d, 2H, J = 7.0 Hz, 4,9-H), 5.27 (s, 4H, 2 x OCH_2), 4.07 (s, 4H, 2 x bridge CH_2), 2.28 (q, 4H, J = 7.5 Hz, 2 x pyrrole-CH_2), 2.18 (s, 6H, 2 x pyrrole-CH_3), 0.73 (t, 6H, J = 7.5 Hz, 2 x CH_2CH_3). ^{13}C NMR (125 MHz, $CDCl_3$): δ 163.2, 138.2, 136.9, 135.1, 132.2, 131.4, 128.3, 127.9, 127.2, 127.1, 125.8, 124.0, 123.2, 122.8, 117.6, 117.5, 65.4, 23.8, 17.5, 16.0, 11.3. ^{13}C NMR (125 MHz, DMSO-d_6): δ 160.8, 137.2, 137.1, 134.2, 131.4, 130.5, 128.6, 127.9, 127.7, 127.6, 126.5, 123.8, 123.7, 122.9, 122.6, 117.7, 116.0, 64.5, 24.0, 16.9, 15.3, 10.4. HR-MS (ESI$^+$) m/z: $[M + H]^+$ calcd for $C_{46}H_{44}N_3O_4$ 702.3332, found: 702.3318.

4.2.3. Bis-1,3-(5-tert-butoxycarbonyl-3-ethyl-4-methyl-2-pyrrolylmethyl)acenaphtho[1,2-c]pyrrole (16a)

Acenaphthopyrrole **29** (0.500 g, 2.62 mmol) and acetoxymethylpyrrole **19a** [40a] (1.47 g, 5.23 mmol) were added to ethanol (30 mL) and acetic acid (2 mL) in a 50 mL round bottom flask. The mixture was purged with nitrogen and stirred under reflux for 16 h. The mixture was poured into ice-water and the resulting precipitate collected by suction filtration, washed with water, and dried *in vacuo*. Recrystallization from chloroform-hexanes gave the tripyrrane (1.17 g, 1.85 mmol, 70%) as a light grey powder, mp 131–132 °C, dec. ^{1}H NMR (500 MHz, $CDCl_3$): δ 8.59 (br s, 2H, 2 x NH), 7.56 (d, 2H, J = 8.2 Hz, 6,7-H), 7.46 (br s, 1H, NH), 7.42 (dd, 2H, J = 6.9, 8.2 Hz, 5,8-H), 7.17 (d, 2H, J = 6.9 Hz, 4,9-H), 4.09 (s, 4H, 2 x bridge-CH_2), 2.42 (q, 4H, J = 7.5 Hz, 2 x CH_2CH_3), 2.28 (s, 6H, 2 x pyrrole-CH_3), 1.48 (s, 18H, 2 x Ot-Bu), 1.01 (t, 6H, J = 7.5 Hz, 2 x CH_2CH_3). ^{13}C NMR (125 MHz, $CDCl_3$): δ 161.5, 138.0, 133.9, 131.2, 138.3, 127.8 (5,8-CH), 126.3, 126.0, 124.5, 123.8 (6,7-CH), 121.2, 119.3, 118.2 (4,9-CH), 80.6 (2 x O–CMe_3), 28.7 (2 x t-Bu), 24.6 (2 x bridge-CH_2), 17.4 2 x CH_2CH_3), 15.7 (2 x CH_2CH_3), 10.7 (2 x pyrrole-CH_3). HR-MS (ESI$^-$) m/z: $[M - H]^-$ calcd for $C_{40}H_{46}N_3O_4^-$ 632.3494, found: 632.3488.

4.2.4. Bis-1,3-(5-tert-butoxycarbonyl-3-ethyl-4-methyl-2-pyrrolylmethyl)phenanthro[9,10-c]pyrrole (20a)

Phenanthropyrrole **18** [20] (400 mg, 1.84 mmol) and acetoxymethylpyrrole **19a** [40a] (1.088 g, 3.87 mmol) were dissolved in ethanol (21 mL), acetic acid (1.4 mL) was added and the mixture was refluxed with stirring under nitrogen for 16 h. The mixture was cooled, poured into ice-water, and the precipitate collected by suction filtration and dried *in vacuo*. Recrystallization from dichloromethane-hexanes gave the phenanthrotripyrrane (1.095 g, 1.66 mmol, 90%) as a white powder, mp 221–223 °C, dec, with softening at 141 °C. ^{1}H NMR (500 MHz, $CDCl_3$): δ 8.51 (d, 2H, J = 8.1 Hz, 7,8-H), 8.50 (br s, 2H, 2 x NH). 8.01 (2H, dd, 2H, J = 1.2, 8.0 Hz, 4,11-H), 7.81 (br s, 1H, NH), 7.50–7.42 (m, 4H, 5,6,9,10-H), 4.41 (s, 4H, 2 x bridge-CH_2), 2.33 (q, 4H, J = 7.5 Hz, 2 x CH_2CH_3), 2.28 (s, 6H, 2 x pyrrole-CH_3), 1.50 (s, 18H, 2 x t-Bu), 0.95 (t, 6H, J = 7.5 Hz, 2 x CH_2CH_3). ^{13}C NMR (125 MHz, $CDCl_3$): δ 161.1, 130.0, 129.5, 127.2 (5,10-CH), 127.0, 126.4, 124.9, 124.8 (6,9-CH), 123.9 (7,8-CH), 123.8 (4,11-CH), 119.8, 118.9, 116.0, 80.6 (2 x $OCMe_3$), 28.7 (2 x t-Bu), 26.5 (2 x bridge-CH_2), 17.4 (2 x CH_2CH_3), 15.4 (2 x CH_2CH_3), 10.7 (2 x pyrrole-Me). HR-MS (EI), m/z: M^+ calcd for $C_{42}H_{49}N_3O_4$ 659.3723, found: 659.3732.

4.2.5. Bis-1,3-(5-tert-butoxycarbonyl-3-(2-methoxycarbonylethyl)-4-methyl-2-pyrrolylmethyl)phenanthro[9,10-c]pyrrole (20b)

Following the previous procedure, phenanthropyrrole **18** [20] (250 mg, 1.15 mmol) was reacted with acetoxymethylpyrrole **19b** [40b] (797 mg, 2.35 mmol) in ethanol (13 mL) and acetic acid (1 mL). Recrystallization from dichloromethane-hexanes gave the tripyrrane (644 mg, 0.831 mmol, 72%) as an off-white or pale yellow solid, mp 135–136 °C, dec. ^{1}H NMR (500 MHz, $CDCl_3$): δ 8.95 (br s, 1H, NH), 8.71 (br s, 2H, 2 x NH). 8.49 (d, 2H, J = 7.9 Hz, 7,8-H), 8.03

(2H, d, 2H, $J = 7.8$ Hz, 4,11-H), 7.47–7.40 (m, 4H, 5,6,9,10-H), 4.50 (s, 4H, 2 x bridge-CH_2), 3.54 (2 x OCH_3), 2.73 (t, 4H, $J = 7.3$ Hz, 2 x pyrrole-CH_2CH$_2$), 2.43 (t, 4H, $J = 7.3$ Hz, 2 x CH_2CO_2), 2.25 (s, 6H, 2 x pyrrole-CH_3), 1.44 (s, 18H, 2 x *t*-Bu). ^{13}C NMR (125 MHz, $CDCl_3$): δ 161.0, 129.9, 129.6, 129.0, 127.3 (5,10-CH), 126.3, 124.8 (6,9-CH), 124.0 (7,8-CH), 123.4 (4,11-CH), 120.0, 119.2, 116.3, 80.6 (2 x $OCMe_3$), 51.8 (2 x OMe), 34.8 (2 x CH_2CO), 28.6 (2 x *t*-Bu), 26.3 (2 x bridge-CH_2), 19.5 (2 x pyrrole-CH_2CH$_2$), 10.7 (2 x pyrrole-Me). HR-MS (ESI$^+$) *m/z*: $[M + H]^+$ calcd for $C_{46}H_{54}N_3O_8$ 776.3911, found: 776.3891.

4.2.6. 7,12,13,18-Tetraethyl-8,17-dimethylphenanthro[9,10-b] porphyrin (22a)

Phenanthrotripyrrane **20a** (100 mg, 0.152 mmol) was stirred with TFA (1 mL) under nitrogen for 5 min. Dichloromethane (15 mL) was added, followed by dialdehyde **21** [44] (27.2 mg, 0.152 mmol), and the mixture was stirred for 2 h. The solution was neutralized by the dropwise addition of triethylamine, DDQ 35.2 mg) was added, and the mixture was stirred for a further 1 h. The solution was washed with dilute sodium bicarbonate solution and evaporated under reduced pressure. The residue was purified on a grade 3 alumina column, eluting with toluene, to give a deep maroon colored fraction. The solvent was removed on a rotary evaporator and the residue recrystallized from chloroform-methanol to give the phenanthroporphyrin (52.4 mg, 0.0873 mmol, 57%) as a red-brown solid, mp > 300 °C. UV–Vis (CH_2Cl_2): λ_{max} ($\log_{10}$ ε) 369 (sh, 4.60), 395 (sh, 4.96), 416 (5.26), 515 (3.92), 554 (4.49), 578 (4.08), 634 (3.43). UV–Vis (2% TFA-CH_2Cl_2): λ_{max} ($\log_{10}$ ε) 403 (sh, 5.04), 420 (5.21), 566 (4.24), 612 (4.30). ^{1}H NMR (500 MHz, $CDCl_3$): δ 11.03 (s, 2H, 5,20-H), 10.03 (s, 2H, 10,15-H), 10.00 (d, 2H, $J = 8.1$ Hz), 9.13 (d, 2H, $J = 8.1$ Hz), 8.13 (t, 2H, $J = 7.5$ Hz), 7.92 (t, 2H, $J = 7.5$ Hz), 4.22 (q, 4H, $J = 7.7$ Hz), 4.03 (q, 4H, $J = 7.7$ Hz), 3.68 (s, 6H), 1.96 (t, 6H, $J = 7.7$ Hz), 1.92 (t, 6H, $J = 7.7$ Hz), −3.60 (br s, 2H, 2 x NH). ^{1}H NMR (500 MHz, TFA-$CDCl_3$): δ 11.50 (s, 2H, 5,20-H), 10.62 (s, 2H, 10,15-H), 9.94 (d, 2H, $J = 8.1$ Hz, 2^1, 3^1-H), 9.29 (d, 2H, $J = 8.2$ Hz, 2^4, 3^4-H), 8.34 (t, 2H, $J = 7.5$ Hz, 2^2, 3^2-H), 8.20 (t, 2H, $J = 7.6$ Hz, 2^3, 3^3-H), 4.20–4.12 (m, 8H, 4 x CH_2CH$_3$), 3.64 (s, 6H, 8,17-CH_3), 1.75 (t, 6H, $J = 7.7$ Hz, 7,18-CH$_2$CH_3), 1.72 (t, 6H, $J = 7.7$ Hz, 12,13-CH$_2$CH_3), −2.88 (br s, 2H), −3.62 (br s, 1H), −3.89 (br s, 1H) (4 x NH). ^{13}C NMR (125 MHz, TFA-$CDCl_3$): δ 144.7, 144.4, 143.2, 142.06, 142.00, 138.1, 138.0, 133.6, 130.2, 129.8 (2^3, 3^3-CH), 129.7 (2^2,3^2-CH), 127.42, 127.36 (2^1, 3^1-CH), 125.2 (2^4, 3^4-CH), 99.9 (5,20-CH), 98.7 (10,15-CH), 20.4, 20.1 (4 x CH_2CH$_3$) 17.3, 16.4 (4 x CH$_2$CH_3), 11.9 (8,17-Me). HR-MS (ESI$^+$) *m/z*: $[M + H]^+$ calcd for $C_{42}H_{41}N_4$ 601.3331, found: 601.3302.

4.2.7. 12,13-Diethyl-7,18-bis(2-methoxycarbonylethyl)-8,17-dimethylphenanthro[9,10-b]porphyrin (21b)

Tripyrrane **20b** (100 mg, 0.129 mmol) was stirred with TFA (1 mL) under nitrogen for 5 min. Dichloromethane (5 mL) was added, followed by dialdehyde **17** (23.1 mg, 0.129 mmol), and the mixture was stirred for 30 min. The solution was diluted with chloroform and shaken with 0.1% aqueous ferric chloride solution for 6–7 min. The chloroform layer was separated and the aqueous solution was back extracted with chloroform. The combined organic solutions were washed with water and 5% sodium bicarbonate, and then evaporated to dryness under reduced pressure. The crude product was run through a grade 3 alumina column, eluting with dichloromethane. Recrystallization from chloroform-methanol gave the porphyrin (30.8 mg, 0.0513 mmol, 34%) as fluffy maroon crystals, mp 244.5–246 °C. UV–Vis (CH_2Cl_2): λ_{max} ($\log_{10}$ ε) 368 (sh, 4.63), 395 (sh, 4.99), 416 (5.28), 514 (4.04), 552 (4.47), 579 (4.06), 635 (3.73). UV–Vis (2% TFA-CH_2Cl_2): λ_{max} ($\log_{10}$ ε) 407 (sh, 5.14), 419 (5.19), 567 (4.27), 611 (4.27). ^{1}H NMR (500 MHz, $CDCl_3$): δ 10.59 (s, 2H, 5,20-H), 9.87 (s, 2H, 10,15-H), 9.81 (d, 2H, $J = 8.1$ Hz, 2^1, 3^1-H), 9.09 (d, 2H, $J = 8.2$ Hz, 2^4, 3^4-H), 8.08 (t, 2H, $J = 7.4$ Hz, 2^2, 3^2-H), 7.92 (t, 2H, $J = 7.4$ Hz, 2^3, 3^3-H), 4.25 (t, 4H, $J = 7.9$ Hz, 7,18-CH_2), 4.00 (q, 4H, $J = 7.7$ Hz, 12,13-CH_2), 3.64 (s, 6H, 2 x OCH_3), 3.55 (s, 6H, 8,17-CH_3), 3.18 (t, 4H, $J = 7.9$ Hz, 2 x CH_2CO_2), 1.92 (t, 6H, $J = 7.7$ Hz, 2 x CH$_2$CH_3), −4.10 (br s, 2H, 2 x NH). ^{1}H NMR (500 MHz, TFA-$CDCl_3$): δ 11.61 (s, 2H, 5,20-H), 10.62 (s, 2H, 10,15-H), 10.02 (d, 2H, $J = 8.1$ Hz, 2^1, 3^1-H), 9.28 (d, 2H, $J = 8.2$ Hz, 2^4, 3^4-H), 8.34 (t, 2H, $J = 7.6$ Hz, 2^2, 3^2-H), 8.20 (t, 2H, $J = 7.6$ Hz, 2^3, 3^3-H), 4.50 (t, 4H, $J = 7.6$ Hz, 7,18-CH_2), 4.13 (q, 4H, 2 x CH_2CH$_3$), 3.69 (s, 6H, 2 x OCH_3), 3.65 (s, 6H, 8,17-CH_3), 3.13 (t, 4H, $J = 7.6$ Hz, 7,18-CH_2), 1.74 (t, 6H, $J = 7.7$ Hz, 2 x CH$_2$CH_3), −2.67 (br s, 2H), −3.45 (br s, 1H), −3.77 (br s, 1H) (4 x NH). ^{13}C NMR (125 MHz, $CDCl_3$): δ 173.5 (C=O), 143.7, 137.0, 134.9, 134.3, 131.9, 129.3, 128.1 (2^2, 3^2-CH), 126.7 (2^1, 3^1-CH), 126.4 (2^3, 3^3-CH), 124.5 (2^4, 3^4-CH), 99.3 (5,20-CH), 97.1 (10,15-CH), 52.0 (2 x OMe), 37.2 (2 x CH_2CO_2Me), 22.2 (7,18-CH_2), 20.0 (12,13-CH_2), 18.8 (2 x CH$_2$CH_3), 11.7 (8,17-Me). ^{13}C NMR (125 MHz, TFA-$CDCl_3$): δ 175.6 (C=O), 144.5, 142.7, 142.1, 142.0, 139.7, 139.2, 138.6, 133.7, 130.5, 129.9 (2^3, 3^3-CH), 129.7 (2^2, 3^2-CH), 127.7 (2^1, 3^1-CH), 127.3, 125.1 (2^4, 3^4-CH), 100.3 (5,20-CH), 99.0 (10,15-CH), 53.2 (2 x OMe), 35.6 (CH_2CO_2Me), 21.9 (7,18-CH_2), 20.1 (12,13-CH_2) 17.3 (2 x CH$_2$CH_3), 12.1 (8,17-Me). HR-MS (ESI$^+$) *m/z*: $[M + H]^+$ calcd for $C_{46}H_{45}N_4O_4$ 717.3441, found 717.3408.

4.2.8. 7,18-Bis(2-methoxycarbonylethyl)-8,17-dimethyldiphenanthro[9,10-b:9.10-l]porphyrin (22)

Prepared by the procedure described for **21b** from phenanthrotripyrrane **20b** (100 mg, 0.129 mmol) and phenanthropyrrole dialdehyde **23** [20] (35.2 mg, 0.129 mmol). The crude product was purified on a grade 3 alumina chromatography column, eluting with dichloromethane, to give a dark green fraction. Recrystallization from chloroform-methanol gave the diphenanthroporphyrin (41.7 mg, 0.0515 mmol, 40%) as dark purple crystals, mp > 300 °C. UV–Vis (1% Et_3N–CH_2Cl_2): λ_{max} ($\log_{10}$ ε) 374 (sh, 4.56), 409 (sh, 5.12), 427 (5.33), 549 (4.14), 573 (4.75), 590 (4.48), 646 (3.59). UV–Vis (2% TFA-CH_2Cl_2): λ_{max} ($\log_{10}$ ε) 407 (sh, 4.86), 437 (5.08), 462 (5.05), 585 (4.31), 634 (4.63). ^{1}H NMR (500 MHz, TFA-$CDCl_3$): δ 11.49 (s, 2H, 5,20-H), 11.37 (s, 2H, 10,15-H), 9.99 (d, 2H, $J = 8.1$ Hz, 2^1, 3^1-H), 9.90 (d, 2H, $J = 8.1$ Hz, 12^1, 13^1-H), 9.28 (d, 4H, $J = 8.2$ Hz, 2^4, 3^4, 12^4, 13^4-H), 8.36–8.31 (m, 4H, 2^2, 3^2, 12^2, 13^2-H), 8.20 (t, 4H, $J = 7.6$ Hz, 2^3, 3^3, 12^3, 13^3-H), 4.43 (t, 4H, $J = 7.6$ Hz, 7,18-CH_2), 3.72 (s, 6H, 2 x OCH_3), 3.64 (s, 6H, 8,17-CH_3), 3.11 (t, 4H, $J = 7.6$ Hz, 7,18-CH_2), −1.60 (br s, 2H), −3.17 (br s, 1H), −3.20 (br s, 1H) (4 x NH). ^{13}C NMR (125 MHz, TFA-$CDCl_3$): δ 175.6 (C=O), 143.3, 142.9, 139.5, 138.9, 138.8, 138.5, 133.72, 133.70, 130.4, 130.3, 129.9, 129.7, 127.7 (2^1, 3^1-CH), 127.4 (12 [1], 13^1-CH), 127.3, 127.2, 125.15, 125.06, 100.4 (10,15-CH), 100.1 (5,20-CH), 53.2 (2 x OMe), 35.6 (CH_2CO_2Me), 21.9 (7,18-CH_2), 12.2 (8,17-Me). HR-MS (ESI$^+$) *m/z*: $[M + H]^+$ calcd for $C_{42}H_{41}N_4$ 811.3284, found: 811.3258.

4.2.9. 8,12,13,17-Tetraethyl-7,18-dimethylphenanthro[9,10-b] porphyrin (24)

Tripyrrane **25** [41,42] (100 mg, 0.22 mmol) was stirred with 1 mL of TFA under nitrogen for 1 min in a 25 mL pear-shaped flask. The solution was diluted with dichloromethane (19 mL) and phenanthropyrrole dialdehyde **23** [20] (60 mg, 0.22 mmol) was immediately added. The mixture was stirred under nitrogen for 2 h. The green solution was neutralized with triethylamine, DDQ (98%, 51 mg, 0.22 mmol) was added and the mixture was stirred for an additional 1 h. The solution was diluted with chloroform, washed with water and evaporated under reduced pressure. The residue was purified on a grade 3 alumina column, eluting with toluene, and a dark maroon fraction was collected. The solvent was removed on a rotary evaporator and the residue recrystallized from chloroform-methanol to give the phenanthroporphyrin (77.4 mg, 0.129 mmol, 58%) as a red-brown solid, mp > 300 °C. UV–Vis (1%

Et_3N–CH_2Cl_2): λ_{max} ($\log_{10}\varepsilon$) 368 (sh, 4.65), 394 (sh, 5.01), 416 (5.31), 515 (4.00), 554 (4.55), 577 (4.15), 633 (3.54). UV–Vis (2% TFA-CH_2Cl_2): λ_{max} ($\log_{10}\varepsilon$) 403 (sh, 5.12), 419 (5.24), 566 (4.28), 612 (4.34). ^{1}H NMR (500 MHz, TFA-$CDCl_3$): δ 11.51 (s, 2H, 5,20-H), 10.61 (s, 2H, 10,15-H), 9.96 (d, 2H, J = 8.2 Hz, 2^1, 3^1-H), 9.28 (d, 2H, J = 8.2 Hz, 2^4, 3^4-H), 8.33 (t, 2H, J = 7.6 Hz, 2^2, 3^2-H), 8.19 (t, 2H, J = 7.7 Hz, 2^3, 3^3-H), 4.18–4.10 (m, 8H, 4 x CH_2CH_3), 3.69 (s, 6H, 7,18-CH_3), 1.76 (t, 6H, J = 7.7 Hz), 1.73 (t, 6H, J = 7.7 Hz) (4 x CH_2CH_3), −2.89 (br s, 2H), −3.61 (br s, 1H), −3.92 (br s, 1H) (4 x NH). ^{13}C NMR (125 MHz, TFA-$CDCl_3$): δ 144.6, 144.3, 142.9, 142.4, 141.9, 138.16, 138.08, 133.6, 130.3, 129.8 (2^3, 3^3-CH), 129.6 (2^2, 3^2-CH), 127.4 (2^1, 3^1-CH), 125.1 (2^4, 3^4-CH), 100.3 (5,20-CH), 98.3 (10,15-CH), 20.3, 20.2 (4 x CH_2CH_3), 17.3, 16.4 (4 x CH_2CH_3), 11.9 (7,18-Me). HR-MS (ESI$^+$) m/z: [M + H]$^+$ calcd for $C_{42}H_{41}N_4$ 601.3331, found 601.3312.

4.2.10. 7,18-Diethyl-8,17-dimethylphenanthro[9,10-b]porphyrin (34)

Prepared by the procedure described for **21a** from tripyrrane **20a** (100 mg, 0.152 mmol) and pyrrole dialdehyde **36** [48] (16.5 mg, 0.151 mmol). The crude product was purified on a grade 3 alumina column, eluting with toluene. Recrystallization from chloroform-methanol gave the porphyrin product (30.3 mg, 0.056 mmol, 37%) as a brick red solid, mp > 300 °C. UV–Vis (CH_2Cl_2): λ_{max} ($\log_{10}\varepsilon$) 413 (5.40), 513 (3.96), 554 (4.51), 575 (4.14), 628 (3.04). UV–Vis (2% TFA-CH_2Cl_2): λ_{max} ($\log_{10}\varepsilon$) 402 (sh, 5.03), 420 (5.23), 525 (sh, 3.51), 565 (4.22), 587 (sh, 3.80), 614 (4.35). ^{1}H NMR (500 MHz, TFA-$CDCl_3$): δ 11.60 (s, 2H, 5,20-H), 10.84 (s, 2H, 10,15-H), 9.96 (d, 2H, J = 8.1 Hz, 2^1, 3^1-H), 9.67 (s, 2H, 12,13-H), 9.32 (d, 2H, J = 8.2 Hz, 2^4, 3^4-H), 8.36 (t, 2H, J = 7.5 Hz, 2^2, 3^2-H), 8.22 (t, 2H, J = 7.6 Hz, 2^3, 3^3-H), 4.23 (q, 4H, J = 7.8 Hz, 2 x CH_2CH_3), 3.68 (s, 6H, 8,17-CH_3), 1.76 (t, 6H, J = 7.8 Hz, 2 x CH_2CH_3), −3.17 (br s, 2H), −3.63 (br s, 2H) (4 x NH). ^{13}C NMR (125 MHz, TFA-$CDCl_3$): δ 144.9, 143.21, 143.18, 142.7, 139.5, 139.1, 133.9, 130.7, 130.5 (12,13-CH), 130.1 (2^3, 3^3-CH), 129.9 (2^2, 3^2-CH), 127.4, 127.3 (2^1, 3^1-CH), 125.3 (2^4, 3^4-CH), 102.8 (10,15-CH), 100.0 (5,20-CH), 20.5 (2 x CH_2CH_3) 16.3 (2 x CH_2CH_3), 11.8 (8,17-Me). HR-MS (EI) m/z: M$^+$ calcd for $C_{38}H_{32}N_4$ 544.2627, found 544.2621.

4.2.11. 8,17-Diethyl-7,18-dimethylphenanthro[9,10-l]-21-oxaporphyrin (32a)

Tripyrrane **20a** (100 mg, 0.152 mmol) was stirred with TFA (5 mL) under nitrogen for 5 min in a 25 mL pear-shaped flask. The solution was diluted with dichloromethane (10 mL), furan dialdehyde **37a** [49] (18.8 mg, 0.152 mmol) was added, and the resulting mixture was stirred for 2 h. The mixture was diluted with chloroform and vigorously shaken with 0.1% aqueous ferric chloride solution (150 mL) for 5 min. The chloroform layer was separated, the aqueous solution back extracted with chloroform, and the combined organic solution washed with 5% sodium bicarbonate. The solvent was evaporated under reduced pressure. Insoluble material that stuck to the glass was dissolved in acetone and combined with the residue. Following recrystallization from chloroform-hexanes, the solid was collected by suction filtration and washed with dichloromethane to give the oxaporphyrin (45.1 mg, 0.0827 mmol, 54%) as dark purple crystals, mp > 300 °C. UV–Vis (1% Et_3N–$CHCl_3$): λ_{max} ($\log_{10}\varepsilon$) 392 (sh, 4.73), 422 (4.83), 508 (3.96), 534 (3.85), 587 (3.71), 630 (3.84), 662 (3.63). UV–Vis (1% TFA-$CHCl_3$): λ_{max} ($\log_{10}\varepsilon$) 386 (5.01), 416 (5.04), 553 (3.98), 593 (4.26). UV–Vis (50% TFA-$CHCl_3$): λ_{max} ($\log_{10}\varepsilon$) 334 (4.12), 397 (5.15), 546 (3.97), 574 (4.04), 625 (4.04). ^{1}H NMR (500 MHz, 10 μL TFA-$CDCl_3$): δ 11.79 (s, 2H, 10,15-H), 11.01 (s, 2H, 5,20-H), 10.48 (s, 2H, 12,13-H), 9.94 (d, 2H, J = 8.1 Hz, 12^1, 13^1-H), 9.28 (d, 2H, J = 8.3 Hz, 12^4, 13^4-H), 8.35 (t, 2H, J = 7.6 Hz, 12^2, 13^2-H), 8.20 (t, 2H, J = 7.6 Hz, 12^3, 13^3-H), 4.31 (q, 4H, J = 7.7 Hz, 2 x CH_2CH_3), 3.79 (s, 6H, 7,18-CH_3), 1.96 (t, 6H, J = 7.7 Hz, 2 x CH_2CH_3). ^{1}H NMR (500 MHz, TFA-$CDCl_3$): δ 11.89 (s, 2H, 10,15-H), 11.13 (s, 2H, 5,20-H), 10.56 (s, 2H, 2,3-H), 9.98 (d, 2H, J = 8.1 Hz, 12^1, 13^1-H), 9.34 (d, 2H, J = 8.2 Hz, 12^4, 13^4-H), 8.40 (t, 2H, J = 7.5 Hz, 12^2, 13^2-H), 8.26 (t, 2H, J = 7.6 Hz, 12^3, 13^3-H), 4.36 (q, 4H, J = 7.5 Hz, 2 x CH_2CH_3), 3.81 (s, 6H, 7,18-CH_3), 1.91 (t, 6H, J = 7.5 Hz, 2 x CH_2CH_3), −3.33 (br s, 2H). ^{13}C NMR (125 MHz, TFA-$CDCl_3$): δ 155.5, 147.2, 143.3, 141.8, 141.0, 140.2, 134.1, 133.8 (2,3-CH), 131.6, 130.6 (12 [3], 13^3-CH), 130.2 (12 [2], 13^2-CH), 127.2 (12 [1], 13^1-CH), 125.5 (12 [4], 13^4-CH), 102.4 (10,15-CH), 100.5 (5,20-CH), 20.7 (2 x CH_2CH_3) 16.8 (2 x CH_2CH_3), 11.9 (8,17-Me). HR-MS (FAB) m/z: [M + H]$^+$ calcd for $C_{38}H_{32}N_3O$ 546.2545, found 546.2544.

4.2.12. 8,17-Diethyl-7,18-dimethylphenanthro[9,10-l]-21-thiaporphyrin (32b)

Tripyrrane **20a** (100 mg, 0.152 mmol) was stirred with TFA (1 mL) under nitrogen for 5 min in a 25 mL pear-shaped flask. The solution was diluted with dichloromethane (10 mL), thiophene dialdehyde **37b** (21.3 mg, 0.152 mmol) was added, and the resulting mixture was stirred for 2 h at room temperature. The mixture was diluted with chloroform and shaken with 0.1% aqueous ferric chloride solution (150 mL) for 5 min. The chloroform layer was separated, the aqueous solution back extracted with chloroform, and the combined organic solutions washed with 5% sodium bicarbonate. The organic layer was evaporated under reduced pressure and the residue purified by column chromatography on grade 3 alumina, eluting with 60% dichloromethane-hexanes. The product was collected as an orange-brown fraction. Recrystallization from chloroform-methanol gave the thiaporphyrin (32.6 mg, 0.0581 mmol, 38%) as a dark solid, mp > 300 °C. UV–Vis (1% Et_3N–CH_2Cl_2): λ_{max} ($\log_{10}\varepsilon$) 422 (5.09), 513 (4.35), 540 (4.04), 607 (3.70), 669 (3.96). UV–Vis (5 equiv TFA-CH_2Cl_2): λ_{max} ($\log_{10}\varepsilon$) 401 (4.98), 431 (5.12), 571 (4.11), 611 (4.16). UV–Vis (5% TFA-CH_2Cl_2): λ_{max} ($\log_{10}\varepsilon$) 334 (4.27), 421 (4.99), 447 (sh, 4.87), 571 (4.08), 597 (4.15), 647 (3.80). ^{1}H NMR (500 MHz, TFA-$CDCl_3$): δ 11.79 (s, 2H, 10,15-H), 11.58 (s, 2H, 5,20-H), 10.52 (s, 2H, 2,3-H), 9.97 (d, 2H, J = 8.1 Hz, 12^1, 13^1-H), 9.37 (d, 2H, J = 8.2 Hz, 12^4, 13^4-H), 8.42 (t, 2H, J = 7.5 Hz, 12^2, 13^2-H), 8.30 (t, 2H, J = 7.6 Hz, 12^3, 13^3-H), 4.23 (q, 4H, J = 7.8 Hz, 2 x CH_2CH_3), 3.76 (s, 6H, 7,18-CH_3), 1.87 (t, 6H, J = 7.8 Hz, 2 x CH_2CH_3). ^{13}C NMR (125 MHz, TFA-$CDCl_3$): δ 150.7, 146.54, 146.49. 145.7, 142.8, 141.3, 139.1 (2,3-CH), 134.3, 132.1, 130.7 (12 [3], 13^3-CH), 130.3 (12 [2], 13^2-CH), 127.6 (12 [1], 13^1-CH), 126.8, 125.5 (12 [4], 13^4-CH), 115.4 (5,20-CH), 102.1 (10,15-CH), 20.5 (2 x CH_2CH_3) 16.4 (2 x CH_2CH_3), 12.0 (8,17-Me). HR-MS (FAB) m/z: [M + H]$^+$ calcd for $C_{38}H_{32}N_3S$ 562.2317, found 562.2317.

4.2.13. 8,17-Diethyl-7,18-dimethylphenanthro[9,10-l]-21-selenaporphyrin (32c)

Selenophene dialdehyde **37c** [50] (28.0 mg, 0.15 mmol) was reacted with tripyrrane **20a** (100 mg, 0.152 mmol) under the foregoing conditions. Recrystallization from chloroform-methanol gave the selenaporphyrin (27.5 mg, 0.452 mmol, 30%) as a dark solid, mp > 300 °C. UV–Vis (1% Et_3N–$CHCl_3$): λ_{max} ($\log_{10}\varepsilon$) 428 (5.01), 519 (4.28), 549 (4.18), 610 (3.74), 619 (sh, 3.70), 672 (3.97). UV–Vis (1% TFA-$CHCl_3$): λ_{max} ($\log_{10}\varepsilon$) 447 (4.85), 488 (sh, 4.53), 590 (4.06), 611 (sh, 4.05), 631 (sh, 3.98), 657 (sh, 3.79). UV–Vis (20% TFA-$CHCl_3$): λ_{max} ($\log_{10}\varepsilon$) 344 (4.33), 402 (4.73), 419 (sh, 4.70), 486 4.73), 591 (sh, 4.10), 617 (4.16). ^{1}H NMR (500 MHz, TFA-$CDCl_3$): δ 11.68 (s, 2H, 10,15-H), 11.60 (s, 2H, 5,20-H), 10.17 (s, 2H, 2,3-H), 9.90 (d, 2H, J = 8.1 Hz, 12^1,13^1-H), 9.34 (d, 2H, J = 8.2 Hz, 12^4,13^4-H), 8.38 (t, 2H, J = 7.5 Hz, 12^2,13^2-H), 8.27 (t, 2H, J = 7.6 Hz, 12^3,13^3-H), 4.25 (q, 4H, J = 7.8 Hz, 2 x CH_2CH_3), 3.76 (s, 6H, 7,18-CH_3), 1.91 (t, 6H, J = 7.8 Hz, 2 x CH_2CH_3). ^{13}C NMR (125 MHz, TFA-$CDCl_3$): δ 148.7, 147.5, 145.2. 142.8, 140.8, 138.3 (2,3-CH), 134.3, 131.9, 130.6 (12 [3],13^3-CH), 130.2 (12 [2],13^2-CH), 127.4 (12 [1],13^1-CH), 126.8, 125.5

(12 [4],13^4-CH), 119.3 (5,20-CH), 101.7 (10,15-CH), 20.5 (2 x CH_2CH_3) 16.4 (2 x CH_2CH_3), 12.0 (8,17-Me). HR-MS (FAB) *m/z*: $[M + H]^+$ calcd for $C_{38}H_{32}N_3Se$ 610.1761, found 610.1763.

4.2.14. 7,18-Diethyl-8,17-dimethylacenaphtho[1,2-b]porphyrin (35)

Acenaphthotripyrrane **16a** [20] (100 mg, 0.158 mmol) was stirred with TFA (2 mL) under nitrogen for 5 min. The solution was diluted with dichloromethane (38 mL) and pyrrole dialdehyde **36** [48] (19.6 mg, 0.159 mmol) was immediately added. The mixture was stirred under nitrogen in the dark overnight. Triethylamine was added dropwise to neutralize the solution, DDQ (46.7 mg) was added, and the mixture stirred for an additional 1 h. The resulting solution was washed with water and the solvent removed *in vacuo*. The residue was purified on a grade 3 alumina column, eluting with dichloromethane. The product fraction was evaporated and the residue recrystallized from chloroform-methanol to give the acenaphthoporphyrin (28.6 mg, 0.0552 mmol, 35%) as a dark powder, mp > 300 °C. UV−Vis ($CHCl_3$): λ_{max} ($\log_{10}\varepsilon$) 387 (4.72), 424 (5.03), 524 (3.93), 568 (4.32), 583 (4.17), 658 (4.03). UV−Vis (50 equiv TFA-$CHCl_3$): λ_{max} ($\log_{10}\varepsilon$) 418 (sh, 4.93), 442 (5.20), 535 (sh, 3.55), 559 (3.97), 600 (3.66), 627 (4.52). UV−Vis (2% TFA-$CHCl_3$): λ_{max} ($\log_{10}\varepsilon$) 358 (sh, 4.51), 435 (5.13), 536 (sh, 3.69), 559 (4.03), 602 (3.75), 627 (4.53). ^{1}H NMR (500 MHz, $CDCl_3$): δ 10.41 (s, 2H, 5,20-H), 10.08 (s, 2H, 10,15-H), 9.36 (s, 2H, 12,13-H), 8.87 (d, 2H, J = 6.6 Hz, 2^1, 3^1-H), 8.04 (d, 2H, J = 8.1 Hz, 2^3, 3^3-H), 7.94 (t, 2H, J = 7.4 Hz, 2^2, 3^2-H), 4.14 (q, 4H, J = 7.7 Hz, 2 x CH_2CH_3), 3.63 (s, 6H, 8,17-CH_3), 1.94 (t, 6H, J = 7.7 Hz, 2 x CH_2CH_3), −3.49 (br s, 2H), −3.58 (br s, 2H) (4 x NH). ^{1}H NMR (500 MHz, TFA-$CDCl_3$, 50 °C): δ 11.17 (s, 2H, 5,20-H), 10.82 (s, 2H, 10,15-H), 9.67 (s, 2H, 12,13-H), 9.17 (d, 2H, J = 6.9 Hz, 2^1, 3^1-H), 8.34 (d, 2H, J = 8.0 Hz, 2^3, 3^3-H), 8.15 (dd, 2H, J = 6.9, 8.0 Hz, 2^2, 3^2-H), 4.27 (q, 4H, J = 7.8 Hz, 2 x CH_2CH_3), 3.72 (s, 6H, 8,17-CH_3), 1.86 (t, 6H, J = 7.8 Hz, 2 x CH_2CH_3), −3.49 (br s, 2H), −3.58 (br s, 2H) (4 x NH). ^{13}C NMR (125 MHz, TFA-$CDCl_3$): δ 145.4, 144.6, 143.2, 143.1, 142.8, 139.4, 136.8, 136.4, 131.5 (2^3, 3^3-CH), 131.3, 131.1, 130.6 (12,13-CH), 129.4 (2^2, 3^2-CH), 127.3 (2^1, 3^1-CH), 102.9 (10,15-CH), 100.6 (5,20-CH), 20.5 (2 x CH_2CH_3) 16.6 (2 x CH_2CH_3), 11.9 (8,17-Me). HR-MS (EI) *m/z*: M^+ calcd for $C_{36}H_{30}N_4$ 518.2470, found 518.2468.

4.2.15. 8,17-Diethyl-7,18-dimethylacenaphtho[1,2-l]-21-oxaporphyrin (33a)

Acenaphthotripyrrane **16a** [20] (100 mg, 0.158 mmol) was stirred with TFA (2 mL) under nitrogen for 5 min. The solution was diluted with dichloromethane (150 mL) and furan dialdehyde **37a** [49] (19.6 mg, 0.158 mmol) was immediately added. The mixture was stirred under nitrogen in the dark for 2 h. The mixture was vigorously shaken with 0.1% aqueous ferric chloride solution (150 mL) for 5 min. The chloroform layer was separated, the aqueous solution back extracted with chloroform, and the combined organic solutions washed with 5% sodium bicarbonate. The organic layer was evaporated under reduced pressure and the residue purified by column chromatography on grade 3 alumina, eluting with 1% triethylamine-dichloromethane and then with 5−10% methanol. The sample was recrystallized from chloroform-hexanes and washed with dichloromethane to give the oxaporphyrin (52.8 mg, 0,192 mmol, 64%) as a dark solid, mp > 300 °C. UV−Vis (1% Et_3N−CH_2Cl_2): λ_{max} ($\log_{10}\varepsilon$) 383 (4.97), 429 (4.83), 454 (4.89), 506 (sh, 4.31), 520 (4.45), 612 (3.77), 621 (3.79), 647 (3.40), 677 (4.50). UV−Vis (5 equiv TFA-CH_2Cl_2): λ_{max} ($\log_{10}\varepsilon$) 355 (4.55), 404 (sh, 4.89), 424 (5.21), 557 (4.04), 605 (4.30). UV−Vis (1% TFA-CH_2Cl_2): λ_{max} ($\log_{10}\varepsilon$) 355 (sh, 4.51), 383 (sh, 4.70), 402 (4.75), 425 (4.92), 459 (sh, 4.71), 551 (4.03), 584 (4.03), 639 (4.28). ^{1}H NMR (500 MHz, TFA-$CDCl_3$): δ 11.54 (s, 2H, 10,15-H), 11.18 (s, 2H, 5,20-H), 10.61 (s, 2H, 2,3-H), 9.29 (d, 2H, J = 7.0 Hz, 12^1, 13^1-H), 8.44 (d, 2H, J = 8.1 Hz, 12^3, 13^3-H), 8.22 (dd, 2H, J = 7.0, 8.1 Hz, 12^2, 13^2-H), 4.42 (q, 4H, J = 7.8 Hz, 2 x CH_2CH_3), 3.87 (s, 6H, 7,18-CH_3), 2.01 (t, 6H, J = 7.8 Hz, 2 x CH_2CH_3), −4.19 (br s, 2H, 2 x NH). ^{13}C NMR (125 MHz, TFA-$CDCl_3$): δ 156.0, 148.3. 146.0, 142.8, 142.2, 141.4, 137.5, 137.2, 134.5 (2,3-CH), 132.7 (12 [3], 13^3-CH), 131.4, 130.6, 129.9 (12 [2], 13^2-CH), 128.1 (12 [1], 13^1-CH), 103.8 (10,15-CH), 100.6 (5,20-CH), 20.7 (2 x CH_2CH_3) 16.8 (2 x CH_2CH_3), 11.8 (8,17-Me). HR-MS (FAB) *m/z*: $[M + H]^+$ calcd for $C_{36}H_{30}N_3O$ 520.2389, found 520.2388.

4.2.16. 8,17-Diethyl-7,18-dimethylacenaphtho[1,2-l]-21-thiaporphyrin (33b)

Acenaphthotripyrrane **16a** [20] (100 mg, 0.158 mmol) was stirred with TFA (2 mL) in a 200 mL pear-shaped flask under nitrogen for 5 min. The solution was diluted with dichloromethane (150 mL) and thiophene dialdehyde **37b** (22.1 mg, 0.158 mmol) was immediately added. The mixture was stirred under nitrogen for 2 h. The solution was shaken with 0.1% aqueous ferric chloride solution (200 mL) for 6 min, the organic phase was separated, and the aqueous solution was back extracted with chloroform. The combined organic solutions were washed with 5% sodium bicarbonate and evaporated under reduced pressure. The residue was purified by column chromatography on grade 3 alumina, eluting with 1% triethylamine-dichloromethane. Recrystallization from chloroform-methanol gave the thiaporphyrin (24.2 mg, 0.0452 mmol, 28%) as a dark solid, mp > 300 °C. UV−Vis (1% Et_3N−CH_2Cl_2): λ_{max} ($\log_{10}\varepsilon$) 313 (4.18), 389 (4.74), 432 (4.75), 456 (4.82), 512 (sh, 4.20), 523 (4,32), 617 (3.66), 626 (3.63), 682 (4.23). UV−Vis (50 equiv TFA-CH_2Cl_2): λ_{max} ($\log_{10}\varepsilon$) 438 (5.08), 564 (4.04), 616 (4.08), 663 (3.83). UV−Vis (1% TFA-CH_2Cl_2): λ_{max} ($\log_{10}\varepsilon$) 415 (4.65), 465 (4.82), 575 (4.08), 607 (4.12), 661 (3.98). UV−Vis (5% TFA-CH_2Cl_2): λ_{max} ($\log_{10}\varepsilon$) 414 (4.66), 472 (4.83), 576 (4.09), 607 (4.14), 661 (3.99). ^{1}H NMR (500 MHz, TFA-$CDCl_3$): δ 11.65 (s, 2H, 5,20-H), 11.50 (s, 2H, 10,15-H), 10.60 (s, 2H, 2,3-H), 9.34 (d, 2H, J = 7.0 Hz, 12^1, 13^1-H), 8.47 (d, 2H, J = 8.1 Hz, 12^3, 13^3-H), 8.25 (dd, 2H, J = 7.0, 8.1 Hz, 12^2, 13^2-H), 4.35 (q, 4H, J = 7.8 Hz, 2 x CH_2CH_3), 3.83 (s, 6H, 7,18-CH_3), 1.97 (t, 6H, J = 7.8 Hz, 2 x CH_2CH_3). ^{13}C NMR (125 MHz, TFA-$CDCl_3$): δ 150.7, 147.8. 146.9, 146.6, 145.1, 143.1, 139.7 (2,3-CH), 138.1, 137.0, 132.9 (12 [3], 13^3-CH), 131.4, 130.6, 129.9 (12 [2], 13^2-CH), 128.1 (12 [1], 13^1-CH), 115.5 (5,20-CH), 103.5 (10,15-CH), 20.5 (2 x CH_2CH_3) 16.6 (2 x CH_2CH_3), 12.0 (8,17-Me). HR-MS (EI) *m/z*: M^+ calcd for $C_{36}H_{29}N_3S$ 535.2082, found 535.2090.

4.2.17. 8,17-Diethyl-7,18-dimethylacenaphtho[1,2-l]-21-selenaporphyrin (33c)

Selenophene dialdehyde **37c** [50] (29.5 mg, 0.158 mmol) was reacted with tripyrrane **16a** under the foregoing conditions. The crude product was purified by column chromatography on grade 3 alumina, eluting with 1% triethylamine-dichloromethane, and then silica eluting with the same solvent mixture. Recrystallization from chloroform-methanol gave the selenaporphyrin (20.9 mg, 0.0359 mmol, 23%) as a dark solid, mp > 300 °C. UV−Vis (1% Et_3N−$CHCl_3$): λ_{max} ($\log_{10}\varepsilon$) 389 (4.55), 435 (sh, 4.71), 457 (4.76), 525 (4.34), 552 (sh, 3.93), 619 (3.80), 628 (3.76), 684 (4.16). UV−Vis (1% TFA-$CHCl_3$): λ_{max} ($\log_{10}\varepsilon$) 386 (sh, 4.45), 464 (4.72), 492 (sh, 4.57), 596 (4.13), 609 (sh, 4.12), 619 (sh, 4.10), 668 (4.01), 727 (3.80). UV−Vis (5% TFA-$CHCl_3$): λ_{max} ($\log_{10}\varepsilon$) 389 (sh, 4.52), 415 (4.53), 494 (4.78), 627 (4.16), 683 (sh, 3.90), 731 (3.74). ^{1}H NMR (500 MHz, TFA-$CDCl_3$): δ 11.66 (s, 2H, 5,20-H), 11.35 (s, 2H, 10,15-H), 10.32 (s, 2H, 2,3-H), 9.28 (d, 2H, J = 7.0 Hz, 12^1,13^1-H), 8.44 (d, 2H, J = 8.1 Hz, 12^3,13^3-H), 8.22 (dd, 2H, J = 7.0, 8.1 Hz, 12^2,13^2-H), 4.33 (q, 4H, J = 7.8 Hz, 2 x CH_2CH_3), 3.80 (s, 6H, 7,18-CH_3), 1.99 (t, 6H, J = 7.8 Hz, 2 x CH_2CH_3). ^{13}C NMR (125 MHz, TFA-$CDCl_3$): δ 148.8, 148.7, 146.6. 144.5, 142.8, 139.4 (2,3-CH), 137.5, 137.0, 132.7 (12 [3],13^3-CH), 131.3, 130.6, 129.8 (12 [2],13^2-CH), 127.9 (12 [1],13^1-CH), 119.4 (5,20-CH), 102.9 (10,15-CH), 20.5 (2 x CH_2CH_3) 16.6 (2 x CH_2CH_3), 12.0 (8,17-Me). HR-MS (EI) *m/z*: M^+ calcd for $C_{36}H_{29}N_3Se$ 583.1527, found 583.1536.

Declaration of competing interest

The authors declare that they have no known competing financial interests or personal relationships that could have appeared to influence the work reported in this paper.

Acknowledgements

This work was supported by the National Science Foundation (CHE-1855240) and the Petroleum Research Fund, administered by the American Chemical Society. PJR also acknowledges additional support from the Beckman Scholars Program.

Appendix A. Supplementary data

Supplementary data to this article can be found online at https://doi.org/10.1016/j.tet.2021.132481.

Supporting information

Selected MS, ^{1}H NMR, ^{1}H–^{1}H COSY, HSQC, DEPT-135, ^{13}C NMR, and UV–Vis spectra are provided.

References

[1] a R. Bonnett, Chem. Soc. Rev. 24 (1995) 19–33;
b M. Ethirajan, Y. Chen, P. Joshi, R.K. Pandey, Chem. Soc. Rev. 40 (2011) 340–362.
[2] a L.L. Li, E.W.G. Diau, Chem. Soc. Rev. 42 (2013) 291–304;
b R. Paolesse, S. Nardis, D. Monti, M. Stefanelli, R.G. Natale, Chem. Rev. 117 (2017) 2517–2583.
[3] T.D. Lash, in: K.M. Kadish, K.M. Smith, R. Guilard (Eds.), The Porphyrin Handbook, vol. 2, Academic Press, San Diego, CA, 2000, pp. 125–199.
[4] T.D. Lash, J. Porphyr. Phthalocyanines 5 (2001) 267–288.
[5] N. Ono, H. Yamada, T. Okujima, in: K.M. Smith, K.M. Kadish, R. Guilard (Eds.), Handbook of Porphyrin Science - with Applications to Chemistry, Physics, Material Science, Engineering, Biology and Medicine, vol. 2, World Scientific Publ, Singapore, 2010, pp. 1–102.
[6] A.V. Cheprakov, in: K.M. Smith, K.M. Kadish, R. Guilard (Eds.), In Handbook of Porphyrin Science - with Applications to Chemistry, Physics, Material Science, Engineering, Biology and Medicine, vol. 13, World Scientific Publ, Singapore, 2011, pp. 1–149.
[7] a P.S. Clezy, C.J.R. Fookes, A.H. Mirza, Aust. J. Chem. 30 (1977) 1337–1347;
b T.D. Lash, Energy Fuels 7 (1993) 166–171;
c S. Ito, T. Murishima, H. Uno, N. Ono, Chem. Commun. (1998) 1661–1662.
[8] a T.D. Lash, T.J. Roper, Tetrahedron Lett. 35 (1994) 7715–7718;
b T.D. Lash, C.P. Denny, Tetrahedron 51 (1995) 59–66;
c J.M. Manley, T.J. Roper, T.D. Lash, J. Org. Chem. 70 (2005) 874–891.
[9] T.D. Lash, B.H. Novak, Angew. Chem., Int. Ed. Engl. 34 (1995) 683–685.
[10] a T.D. Lash, B.H. Novak, Tetrahedron Lett. 36 (1995) 4381–4384;
b B.H. Novak, T.D. Lash, J. Org. Chem. 63 (1998) 3998–4010.
[11] V. Gandhi, M.L. Thompson, T.D. Lash, Tetrahedron 66 (2010) 1787–1799.
[12] T.D. Lash, T.M. Werner, M.L. Thompson, J.M. Manley, J. Org. Chem. 66 (2001) 3152–3159.
[13] H. Boedigheimer, G.M. Ferrence, T.D. Lash, J. Org. Chem. 75 (2010) 2518–2527.
[14] a T. Okujima, N. Komobuchi, H. Uno, N. Ono, Heterocycles 67 (2006) 255–267;
b T. Okujima, J. Mack, J. Nakamura, G. Kubheka, T. Nyokong, H. Zhu, N. Komobuchi, N. Ono, H. Yamada, H. Uno, N. Kobayashi, Chem. Eur J. 22 (2016) 14730–14738.
[15] S. Ito, N. Ochi, H. Uno, T. Murashima, N. Ono, Chem. Commun. (2000) 893–894.
[16] H. Yamada, D. Kuzuhara, K. Ohkubo, T. Takahashi, T. Okujima, H. Uno, N. Ono, S. Fukuzuni, J. Mater. Chem. 20 (2010) 3011–3024.
[17] T.D. Lash, V. Gandhi, J. Org. Chem. 65 (2000) 8020–8026.
[18] a Y. Lin, T.D. Lash, Tetrahedron Lett. 36 (1995) 9441–9444;
b T.D. Lash, Y. Lin, B.H. Novak, M.D. Parikh, Tetrahedron 61 (2005) 11601–11614.
[19] T.D. Lash, C. Wijesinghe, A.T. Osuma, J.R. Patel, Tetrahedron Lett. 38 (1997) 2031–2034.
[20] T.D. Lash, P. Chandrasekar, A.T. Osuma, S.T. Chaney, J.D. Spence, J. Org. Chem. 63 (1998) 8455–8469.
[21] C.M. Cillo, T.D. Lash, Tetrahedron 61 (2005) 11615–11627.
[22] C.M. Cillo, M.A. Geiger, T.D. Lash, Tetrahedron Lett. 61 (2020) 152576.
[23] P. Chandrasekar, T.D. Lash, Tetrahedron Lett. 37 (1996) 4873–4876.
[24] a T.D. Lash, P. Chandrasekar, J. Am. Chem. Soc. 118 (1996) 8767–8768;
b J.D. Spence, T.D. Lash, J. Org. Chem. 65 (2000) 1530–1539;
c P.J. Rauen, T.D. Lash, Tetrahedron Lett. 61 (2020) 152662.
[25] a T.D. Lash, D.T. Richter, J. Am. Chem. Soc. 120 (1998) 9965–9966;
b D.T. Richter, T.D. Lash, Tetrahedron Lett. 40 (1999) 6735–6738;
c D.T. Richter, T.D. Lash, J. Org. Chem. 69 (2004) 8842–8850. See also: Okujima T, Ando C, Mack J, Mori S, Hisaki I, Nakae T, Yamada H, Ohara K, Kobayashi N, Uno H. Chem. Eur. J. 2013; 41: 13970-13978.
[26] T.D. Lash, M.J. Hayes, J.D. Spence, M.A. Muckey, G.M. Ferrence, L.F. Szczepura, J. Org. Chem. 67 (2002) 4860–4874.
[27] T.D. Lash, S.T. Chaney, D.T. Richter, J. Org. Chem. 63 (1998) 9076–9088.
[28] D.M. Gardner, V.M. Taylor, D.L. Cedeño, S. Padhee, S.M. Robledo, M.A. Jones, T.D. Lash, I.D. Vélez, Photochem. Photobiol. 86 (2010) 645–652.
[29] G. Yang, L. Liu, Q. Yang, S. Wang, Chem. Asian J. 6 (2011) 1147–1150.
[30] a H. Zhylitskaya, J. Cybinska, P. Chmieleewski, T. Lis, M. Stepien, J. Am. Chem. Soc. 138 (2016) 11390–11398;
b S. Kumar, K.M. Maurya, S. Kang, P. Chmielewski, T. Lis, J. Cybinska, D. Kim, M. Stepien, Org. Lett. 22 (2020) 7202–7207.
[31] L. Latos-Grazzynski, in: K.M. Kadish, K.M. Smith, R. Guilard (Eds.), The Porphyrin Handbook, vol. 2, Academic Press, San Diego, 2000, pp. 361–416.
[32] C. Brückner, J. Akhigbe, L.P. Samankumara, in: K.M. Smith, K.M. Kadish, R. Guilard (Eds.), Handbook of Porphyrin Science - with Applications to Chemistry, Physics, Material Science, Engineering, Biology and Medicine, vol. 31, World Scientific, Singapore, 2014, pp. 1–275.
[33] T. Chatterjee, V.S. Shetti, R. Sharma, M. Ravikanth, Chem. Rev. 117 (2017) 3254–3328.
[34] M.J. Broadhurst, R. Grigg, A.W. Johnson, J. Chem. Soc. C (1971) 3681–3690.
[35] T.D. Lash, Chem. Eur J. 2 (1996) 1197–1200.
[36] T.D. Lash, J. Porphyr. Phthalocyanines 20 (2016) 855–888.
[37] A.N. Latham, T.D. Lash, J. Org. Chem. 85 (2020) 13050–13068.
[38] a T.D. Lash, B.H. Novak, Y. Lin, Tetrahedron Lett. 35 (1994) 2493–2494;
b T.D. Lash, M.L. Thompson, T.M. Werner, J.D. Spence, Synlett (2000) 213–216;
c N. Ono, H. Hironaga, K. Ono, S. Kaneko, T. Murashima, T. Ueda, C. Tsukamura, T. Ogawa, J. Chem. Soc., Perkin Trans. 1 (1996) 417–423.
[39] a D.H.R. Barton, S.Z. Zard, J. Chem. Soc., Chem. Commun. 21 (1985) 1098–1100;
b D.H.R. Barton, J. Kervagoret, S.Z. Zard, Tetrahedron 46 (1990) 7587–7598;
c T.D. Lash, J.R. Bellettini, J.A. Bastian, K.B. Couch, Synthesis (1994) 170–172;
d G.W. Gribble, in: J.J. Li (Ed.), In Name Reactions in Heterocyclic Chemistry, Wiley, Hoboken, NJ, 2005, pp. 70–78.
[40] a P.S. Clezy, R.J. Crowley, T.T. Hai, Aust. J. Chem. 35 (1982) 411–421;
b P.S. Clezy, A.J. Liepa, Aust. J. Chem. 23 (1970) 2443–2459.
[41] J.L. Sessler, M.R. Johnson, V. Lynch, J. Org. Chem. 52 (1987) 4394–4397.
[42] T.D. Lash, J. Porphyr. Phthalocyanines 1 (1997) 29–44.
[43] A.H. Jackson, W. Lertwanawatana, R.K. Pandey, K.R.N. Rao, J. Chem. Soc., Perkin Trans. 1 (1989) 374–375.
[44] a C. Tardieux, F. Bolze, C.P. Gros, R. Guilard, Synthesis (1998) 267–268;
b R. Li, A.D. Lammer, G.M. Ferrence, T.D. Lash, J. Org. Chem. 79 (2014) 4078–4093.
[45] H. Iida, I. Kajiyama, K. Yamada, *Nippon kagaku kaishi* 1972: 137, Chem. Abstr. 76 (1972) 99395m.
[46] W. Jiao, T.D. Lash, J. Org. Chem. 68 (2003) 3896–3901.
[47] T.D. Lash, K.M. Bergman, J. Org. Chem. 77 (2012) 9774–9783.
[48] a C.E. Loader, H.J. Anderson, Synthesis (1978) 295–296;
b S. Cadamuro, I. Degani, R. Fochi, A. Gatti, L. Piscopo, J. Chem. Soc., Perkin Trans. 1 (1993) 2939–2943.
[49] B.L. Feringa, R. Hulst, R. Rikers, L. Brandsma, Synthesis (1988) 316–318.
[50] T.D. Lash, D.A. Colby, S.R. Graham, S.T. Chaney, J. Org. Chem. 69 (2004) 8851–8864.
[51] T.D. Lash, D.T. Richter, C.M. Shiner, J. Org. Chem. 64 (1999) 7973–7982.
[52] A.W. Johnson, I.T. Kay, E. Markham, R. Price, K.B. Shaw, J. Chem. Soc. (1959) 3416.